Oxygen, facies, and secular controls on the appearance of Cryogenian and Ediacaran body and trace fossils in the Mackenzie Mountains of northwestern Canada

Erik A. Sperling[1,†], Calla Carbone[2], Justin V. Strauss[1], David T. Johnston[1], Guy M. Narbonne[2,§], and Francis A. Macdonald[1,§]

[1]*Department of Earth and Planetary Sciences, Harvard University, 20 Oxford Street, Cambridge, Massachusetts 02138, USA*
[2]*Department of Geological Sciences and Geological Engineering, Queens University, Kingston, Ontario K7L 3N6, Canada*

ABSTRACT

The causes behind the appearance of abundant macroscopic body and trace fossils at the end of the Neoproterozoic Era remain debated. Iron geochemical data from fossiliferous Ediacaran successions in Newfoundland suggested that the first appearances correlated with an oxygenation event. A similar relationship was claimed to exist in the Mackenzie Mountains, Canada, although later stratigraphic studies indicated that the sections analyzed for geochemistry were incorrectly correlated with those hosting the fossils. To directly connect fossil occurrences with geochemistry in the Mackenzie Mountains, we conducted a multiproxy iron, carbon, sulfur, and trace-element geochemical analysis of stratigraphic sections hosting both the Cryogenian "Twitya discs" at Bluefish Creek as well as Ediacaran fossils and simple bilaterian traces at Sekwi Brook. There is no clear oxygenation event correlated with the appearance of macroscopic body fossils or simple bilaterian burrows; however, some change in environment—a potential partial oxygenation—is correlated with increasing burrow width higher in the Blueflower Formation. Data from Sekwi Brook suggest that these organisms were periodically colonizing a predominantly anoxic and ferruginous basin. This seemingly incongruent observation is accommodated through accounting for differing time scales between the characteristic response time of sedimentary redox proxies versus that for ecological change. Thus, hypotheses directly connecting ocean oxygenation with the appearance of macrofossils need not apply to all areas of a heterogeneous Ediacaran ocean, and stably oxygenated conditions on geological time scales were not required for the appearance of these Avalon-assemblage Ediacaran organisms. At least in the Mackenzie Mountains, the appropriate facies for fossil preservation appears to be the strongest control on the stratigraphic distribution of macrofossils.

INTRODUCTION

The first abundant macroscopic organisms in the fossil record make their appearance toward the end of the Neoproterozoic Era. Ediacara-type impressions, preceded by the appearance of the microscopic remains of multiple eukaryotic groups in the Tonian and early Cryogenian Periods (Knoll, 2014), were followed by the first evidence for bilaterian burrows in the late Ediacaran and ultimately the flowering of animal life during the Cambrian radiation (Droser et al., 1999; Maloof et al., 2010; Erwin et al., 2011; Erwin and Valentine, 2013; Carbone and Narbonne, 2014). Although the phylogenetic affinities of the Ediacara biota are contentious, the organisms are increasingly being viewed as containing members of several disparate eukaryotic groups, united by time and taphonomic mode, rather than representing a single monophyletic clade (reviewed recently by Xiao and Laflamme, 2009; Grazhdankin, 2014). The size and abundance of the Ediacara biota fossils, which are conspicuously absent from taphonomically similar strata of older age, herald an important change in eukaryotic life on the eve of the Cambrian explosion.

This begs the question of why these organisms arose at this point in Earth's history. The answer need not require a single causal factor—a combination of ecological, genomic, and environmental factors was likely at play. Environmental factors have received considerable study in recent years, particularly the temporal relationship between oxygenation of the oceans and the first appearances of these fossils. In an extensive sedimentary geochemistry study of fossiliferous strata of the Conception Group of eastern Newfoundland, Canfield et al. (2007) used iron speciation data to demonstrate that the Mall Bay Formation was deposited under generally anoxic and ferruginous conditions, with more robust evidence for anoxia present near the onset of the ca. 580 Ma Gaskiers glaciation. Anoxic conditions persisted through the deposition of glacial strata and then abruptly changed to oxygenated conditions immediately following the glaciation. This redox change coincides with the first appearance—both in the Conception Group and globally—of macroscopic fossils common to the Ediacara biota (Narbonne and Gehling, 2003). This was then taken as potentially pointing to a causal link between an oxygenation event (local or global) and diversification. Following from that work, other workers have claimed that an oxygenation event in the Sheepbed Formation at the Shale Lake locality in the Mackenzie Mountains of northwestern Canada (Fig. 1) correlates with the first appearance of Ediacaran fossils at Sekwi Brook ~135 km farther south (Shen et al., 2008).

The first step in distinguishing coincidence from correlation is determining whether temporal linkages represent a global pattern, regional events, or simply the unrelated appearance of organisms during a time interval characterized by broadly increasing oxygen levels. Neoproterozoic oxygenation, if present, is increasingly being recognized as regionally heterogeneous (Kah and Bartley, 2011). This is reflected in iron speciation data from the southern Canadian Cordillera showing an increased prevalence of anoxic conditions during the mid-Ediacaran (Canfield et al., 2008), in contrast to the Newfoundland data, and data from the Wernecke Mountains of northwestern Canada,

[†]Current address: Department of Geological Sciences, Stanford University, Stanford, California 94305, USA.
[§]E-mails: narbonne@queensu.ca; fmacdon@fas.harvard.edu.

GSA Bulletin; March/April 2016; v. 128; no. 3/4; p. 558–575; doi: 10.1130/B31329.1; 8 figures; 3 tables; Data Repository item 2015326; published online 5 November 2015.

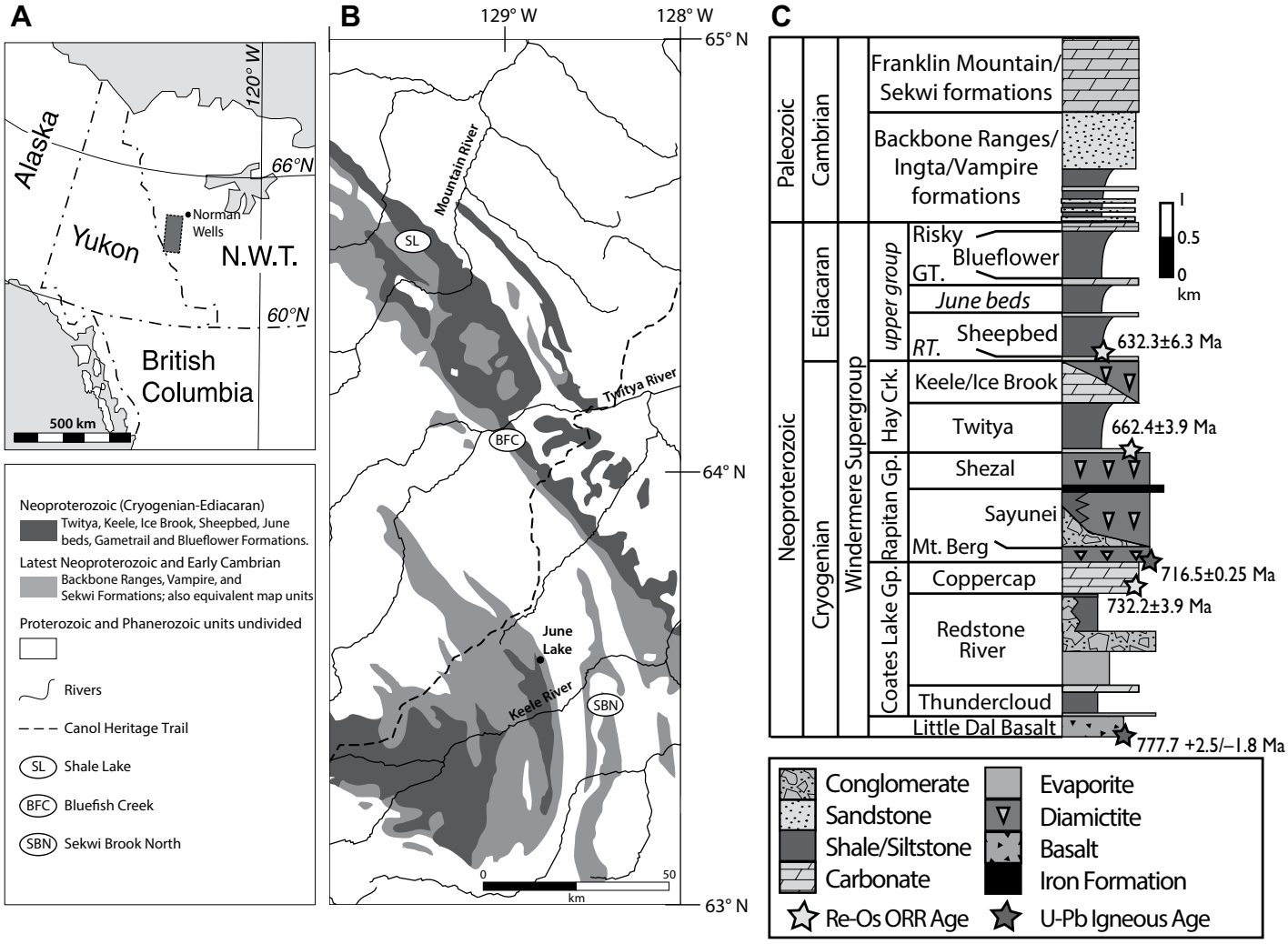

Figure 1. Locality map of investigated Cryogenian and Ediacaran strata in NW Canada. (A) Outline of study region in the Northwest Territories of NW Canada. (B) Distribution of Neoproterozoic–Cambrian strata in the Mackenzie Mountains, Northwest Territories. Sampling localities in this study are Bluefish Creek (BFC) and Sekwi Brook North (SBN). The sedimentary geochemistry of the Ediacaran Sheepbed Formation was sampled at Shale Lake (SL) by Shen et al. (2008) and Canfield et al. (2008). The Ediacaran succession analyzed by Johnston et al. (2013) at the Goz A locality is located ~170 km northwest of Shale Lake (off map) in the Wernecke Mountains, Yukon. Map is modified from MacNaughton et al. (2008). (C) Generalized stratigraphic column of the Windermere Supergroup, Mackenzie Mountains, Northwest Territories. Stratigraphic thicknesses are schematic and vary widely. Italics indicate informally named units. Column is modified from Narbonne and Aitken (1995); Martel et al. (2011); Macdonald et al. (2013); Rooney et al. (2014, 2015). U-Pb age on Little Dal Basalt is from Jefferson and Parish (1989), U-Pb ages from base of Rapitan Group are from Macdonald et al. (2010), and Re-Os ages are from Rooney et al. (2014, 2015). RT.—Ravensthroat, GT.—Gametrail Formation, ORR—organic-rich rock, N.W.T.—Northwest Territories.

which show no change at all (Johnston et al., 2013). Other regions such as Namibia also show heterogeneous but generally anoxic and ferruginous conditions through the late Ediacaran (Wood et al., 2015). Analyzed collectively and statistically, a global database of Proterozoic and Paleozoic iron speciation data shows no overall change to the oxygenation state of marine environments between the Ediacaran and Cambrian (Sperling et al., 2015). These database analyses do not rule out an increase in oxygen through this time period, but they do limit the magnitude of such a change to much less than is normally depicted (e.g., Holland, 2006).

Poor age constraints further complicate the integration of geochemical and ecological patterns, and thus, in many sedimentary successions, inferring the relationship between environmental change and biotic response is dependent on stratigraphic correlation. For example, and central to this contribution, the geochemical data from NW Canada underpinning the hypothesized oxygenation event of Shen et al. (2008) were from unfossiliferous sections of the Sheepbed Formation at the Shale Lake locality (Fig. 1). These data were correlated with the appearance of Ediacaran fossils at Sekwi Brook, in strata that were originally assigned to the Sheepbed Formation (Aitken, 1989). However, Macdonald et al. (2013) demonstrated that the fossiliferous beds were miscorrelated with the Sheepbed Formation of Shale Lake; they actually appear within the informally named June beds, an unconformably overlying stratigraphic package. Thus, tests of the linkage between redox change and macroscopic fossil

first appearances in NW Canada require data directly from the fossiliferous sections.

The geochemical samples in this study were collected during an integrated study of the stratigraphy, paleontology, and geochemistry of Cryogenian and Ediacaran strata in the Mackenzie Mountains. Cryogenian strata were sampled at Bluefish Creek (Fig. 1), which has yielded small discoidal fossils informally known as "Twitya discs" (Figs. 2E–2G; Hofmann et al., 1990). Ediacaran samples were collected from Sekwi Brook, which has yielded diverse assemblages of trace fossils and Ediacara-type body fossils that collectively extend through more than 1 km of stratigraphy (Figs. 2A–2D and 3; Hofmann, 1981; Narbonne and Aitken, 1990, 1995; Narbonne, 1994; Narbonne et al., 2014; Carbone and Narbonne, 2014; Carbone et al., 2015). Fine-grained clastic sediments (shale, calcareous shale, and siltstone) from these sections were analyzed for iron speciation, major- and minor-element composition, redox-sensitive trace-metal abundances, pyrite sulfur isotope values, and total organic carbon contents. Finally, as burrow size has been shown to increase with increasing oxygen level (e.g., Savrda et al., 1984), burrow diameter measurements were collected through the well-developed ichnofaunal record in the Blueflower Formation (McNaughton and Narbonne, 1999; Carbone and Narbonne, 2014). The geochemical data were then compared against the body and trace-fossil record to directly test the relationship between redox state and fossil stratigraphic distribution in the Cryogenian and Ediacaran strata of northwestern Canada.

GEOLOGICAL SETTING

Stratigraphy, Age, and Tectonic Setting

Neoproterozoic strata in northwestern Canada are exposed as a series of inliers among Phanerozoic cover (Gabrielse, 1972). In the Mackenzie Mountains, the Windermere Supergroup, to which the investigated strata belong, is ~6 km thick and consists of the Coates Lake, Rapitan, Hay Creek, and "upper" groups (Martel et al., 2011; Turner et al., 2011). Deposition of these strata spans portions of the Cryogenian and Ediacaran Periods, with an unconformity at the top of the Risky Formation of the upper group broadly marking the Ediacaran-Cambrian boundary (Fig. 1; Narbonne and Aitken, 1995). The Windermere Supergroup begins with the rift-related Coates Lake Group, followed by the Rapitan Group, the base of which has been bracketed in correlative strata in Yukon with U-Pb chemical abrasion–isotope dilution–thermal ionization mass spectrometry (CA-ID-TIMS) on single-grain zircon at 717.43 ± 0.14 Ma (beneath diamictite) and 716.47 ± 0.24 Ma (within diamictite, both ages 2σ), and correlated with Sturtian-age glacial deposits globally (Macdonald et al., 2010). The glaciogenic character of these deposits is indicated by the widespread occurrence of faceted and striated clasts, outsized dropstones with impact-related structures, and sand aggregates ("till pellets"), as well as glacial push structures in the Hart River inlier (reviewed by Hoffman and Halverson, 2011). The Rapitan Group is succeeded by the Cryogenian Twitya, Keele, and Ice Brook formations of the Hay Creek Group. The lower members (Durkan and Delthore) of the Ice Brook Formation are slope equivalents of the Keele Formation (Aitken, 1991). The upper member (Stelfox) of the Ice Brook

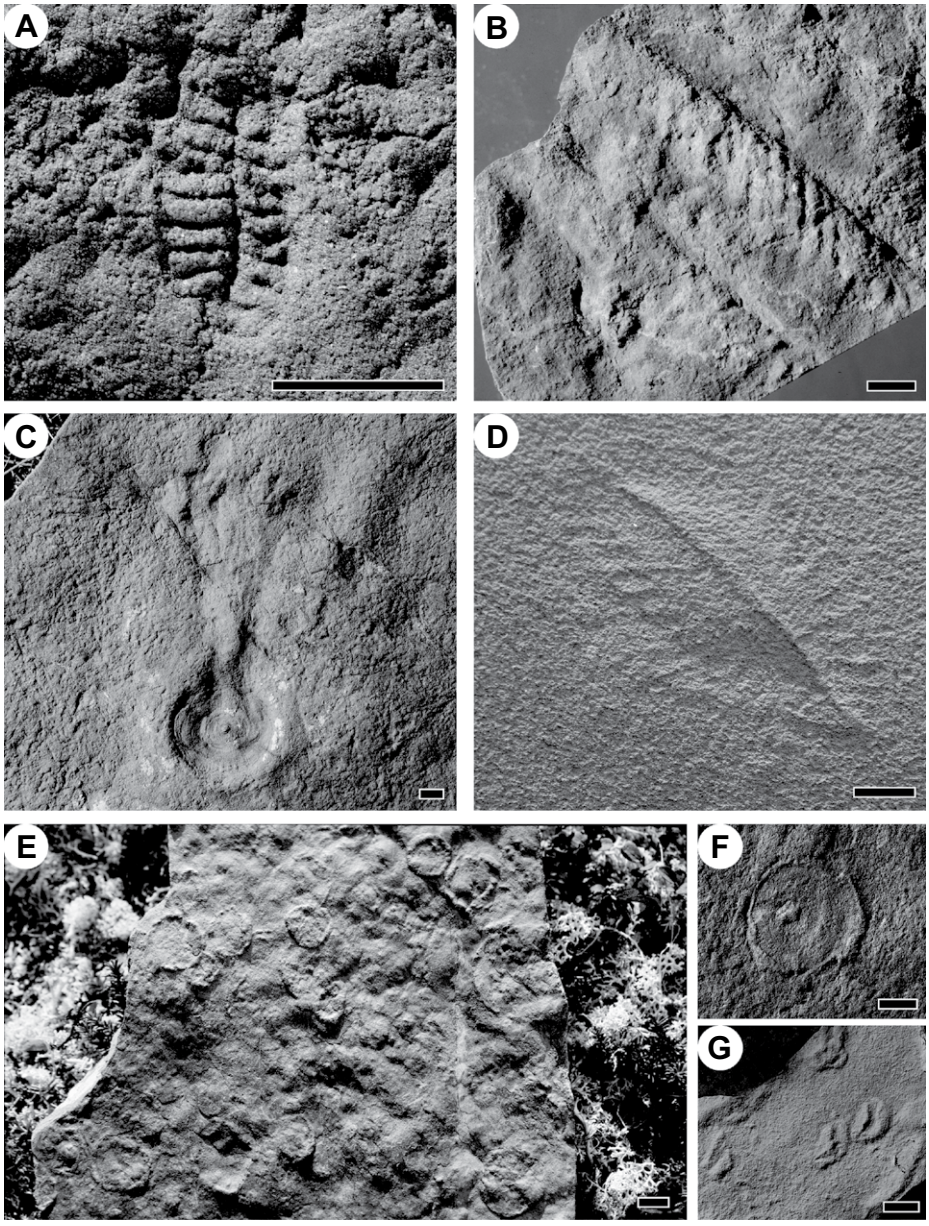

Figure 2. (A–D) Ediacaran soft-bodied fossils from Sekwi Brook and (E–G) "Twitya discs" from Bluefish Creek. Scale bar represents 1 cm. Specimens A–C and E–G are preserved on the soles of turbidite beds; specimen D is a raised feature within a contourite bed. (A) *Windermeria*, a shallow-water dickinsoniomorph from the uppermost Blueflower Formation; (B) *Pterinidinium?*, from the lower Blueflower Formation; (C) *Primocandelabrum*, a deep-water frond attached to a discoid holdfast in the June beds; (D) *Fractofusus*, a deep-water rangeomorph from the June beds; (E–F) discoidal "Twitya discs"; (G) hemispherical "Twitya discs" showing partial overfolding due to current flow.

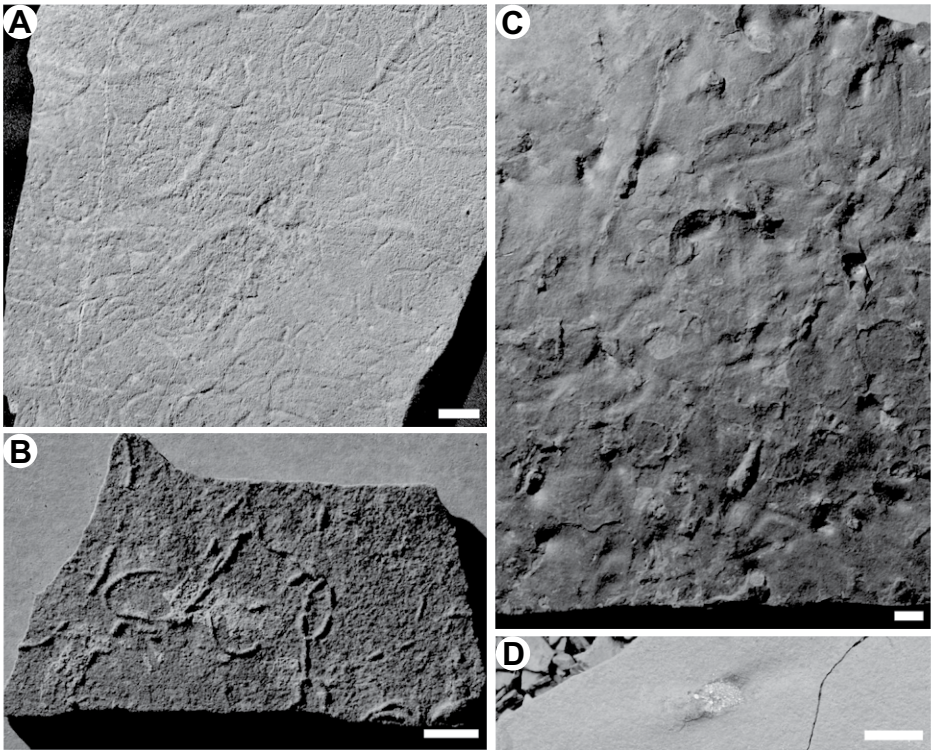

Figure 3. Trace fossils from Blueflower Formation at Sekwi Brook: (A) *Helminthoidichnites* and *Planolites* from the lower Blueflower Formation, (B) *Planolites* from the lower Blueflower, and (C–D) *Palaeophycus* from the upper Blueflower Formation.

Formation contains faceted/striated clasts, dropstones with impact-related structures in finely laminated sediments, till pellets, and diamictites in shallow-shelf settings where large mass flows would not be expected, and it is interpreted as glaciomarine (reviewed by Hofman and Halverson, 2011). The Stelfox Member has been correlated with ca. 635 Ma Marinoan glacial deposits globally and is overlain by the basal Ediacaran Ravensthroat cap carbonate (James et al., 2001; Hoffman and Halverson, 2011; Macdonald et al., 2013). The informal "upper" group begins with shale of the Sheepbed Formation, which has been recently dated with Re-Os geochronology at its base at 632 ± 5.0 Ma (Rooney et al., 2015), confirming previous correlations with early Ediacaran strata. The Sheepbed Formation is succeeded by the newly distinguished and informal June beds (Macdonald et al., 2013). The June beds are followed by the dominantly carbonate Gametrail Formation, mixed carbonate-clastic Blueflower Formation, and dominantly carbonate Risky Formation. The Precambrian-Cambrian boundary is either in the lacuna of the karst horizon at the top of the Risky Formation, or it is preserved in the overlying lower Ingta Formation in more distal sections (Macdonald et al., 2013; MacNaughton and Narbonne, 1999; Carbone and Narbonne, 2014).

Sedimentary rocks of the Coates Lake and Rapitan groups have traditionally been interpreted as rift-related deposits associated with the opening of the proto–Pacific Ocean (e.g., Aitken, 1989; Ross et al., 1989; Ross, 1991; Dalrymple and Narbonne, 1996), with the rift-drift transition generally placed near the base of the Twitya Formation (Narbonne and Aitken, 1995). However, evidence for synsedimentary faulting is present throughout the Coates Lake, Rapitan, Hay Creek, and upper groups in the northern Cordillera, questioning the development of an open, passively subsiding margin (Eisbacher, 1981; Aitken, 1991; Thorkelson, 2000). This suggests a more complicated history for the Cordilleran margin, with distinct Cryogenian and Ediacaran extensional events and final rifting and passive margin development occurring in the mid- to late Ediacaran and Early Cambrian (Macdonald et al., 2013; Yonkee et al., 2014). Support for a mid-Ediacaran to Cambrian rift-drift transition is found in large lateral facies changes in the latest Ediacaran to Early Cambrian strata in both the northern (e.g., Fritz, 1982; Aitken, 1989; Macdonald et al., 2013) and southern (Devlin, 1989; Devlin and Bond, 1988; Lickorish and Simony, 1995) Canadian Cordillera, mid-Ediacaran ages of rift-related volcanism in the Hamill Group of British Columbia (Colpron et al., 2002) and Browns Hole Formation of Utah (Link et al., 1993), and tectonic subsidence analyses (e.g., Bond et al., 1985). Most likely, the investigated Cryogenian Hay Creek Group at Bluefish Creek was deposited in a narrow extensional pull-apart basin with large local topographic relief (Eisbacher, 1981; Jefferson and Ruelle, 1986; Aitken, 1991). This is important in the context of redox geochemistry because smaller basins will be more prone to hydrographic restriction. The identity of the landmass that rifted from the western margin of Laurentia in the Cryogenian to Ediacaran, the size of the basin, and the degree to which this basin was in communication with the open ocean remain uncertain. Nonetheless, marine carbonates, stratigraphic architecture, and probable contourites at Sekwi Brook (Dalrymple and Narbonne, 1996; Narbonne et al., 2014) suggest a substantially open, juvenile marine margin.

In the northern Canadian Cordillera, metamorphic grade generally decreases to the northeast. The Neoproterozoic successions exposed at Bluefish Creek and Sekwi Brook have experienced sub-greenschist-facies metamorphism due to burial and fluid alteration during Mesozoic–Paleogene shortening (Gordey et al., 2011). Just south of the Sekwi area, maximum burial of Neoproterozoic strata was estimated to be less than 10 km (Gordey and Anderson, 1993). This range of burial metamorphic conditions is lower than those in the southern Cordillera and Avalonia, where iron speciation has been previously reported (Canfield et al., 2007, 2008). Regional Mesozoic–Paleozoic fluid alteration resulted in localized carbonate-hosted Pb-Zn mineralization in which metals from crustal sources were carried by basinal brines and were precipitated at 75–200 °C (Gordey et al., 2011). This event likely caused some remobilization of pyrite, which is occasionally present in our sections as oxidized macroscopic cubes; however, fluid flow and mineralization were focused along faults and permeable units rather than in impermeable shale. While sampling, we avoided macroscopic pyrite and other evidence of local fluid flow such as alteration along fractures.

Bluefish Creek Stratigraphic Section

The investigated Cryogenian to Ediacaran exposures at Bluefish Creek span the Shezal Formation of the Rapitan Group, the Twitya and Ice Brook formations of the Hay Creek Group, and the basal Sheepbed Formation of the upper group (Gordey et al., 2011). The base of our measured section (Fig. 4) begins with glacial diamictite of the Shezal Formation. The first 9.5 m section of the overlying Twitya Formation

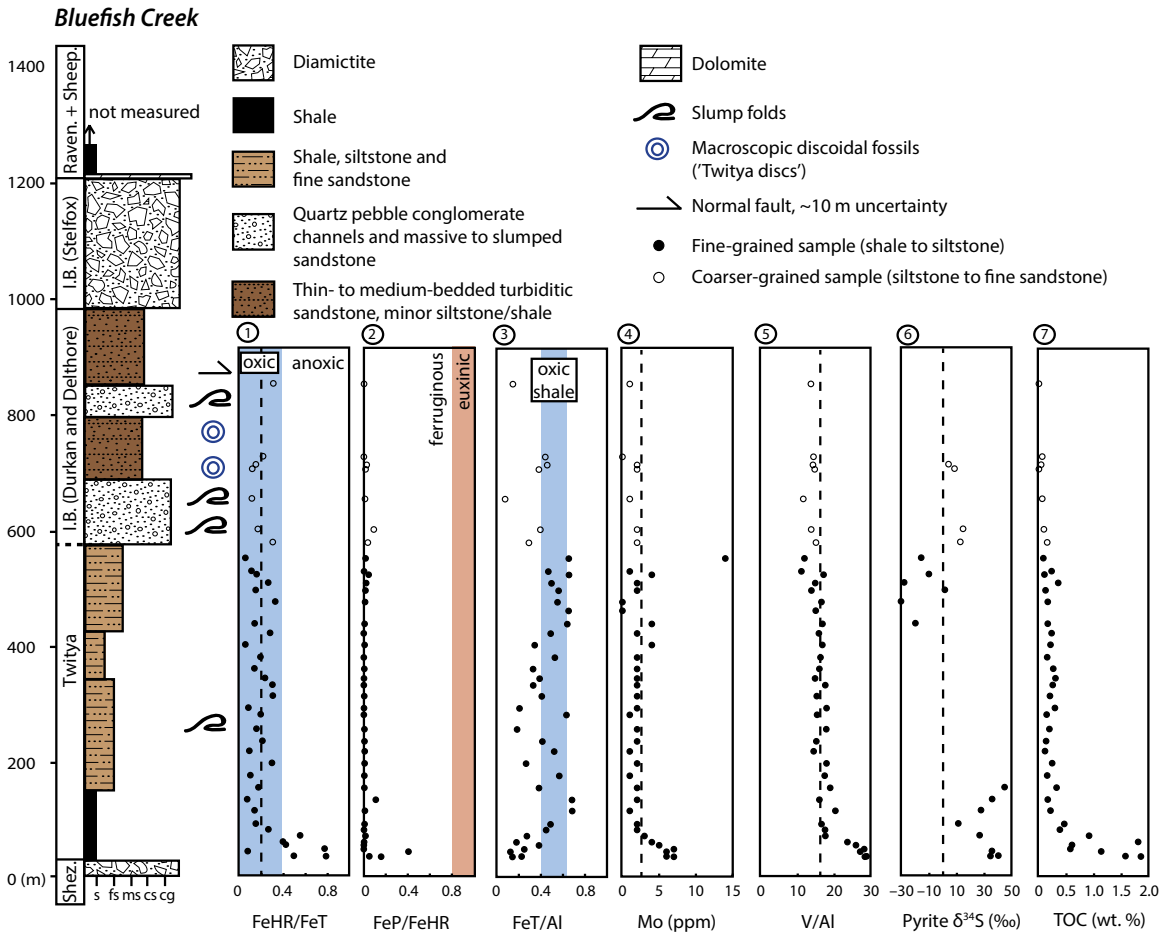

Figure 4. Multiproxy sedimentary geochemistry of the Twitya and Ice Brook Formations at Bluefish Creek. Note that the Ice Brook Formation, which bears the macroscopic discoidal fossils (Hoffmann et al., 1990; Figs. 2E–2G), is mapped at the appearance of deep-water quartz pebble-conglomerate channels and slumped sands (Gordey et al., 2011). Due to uncertainty about facies change in the Twitya in slope localities, this correlation is imprecise, and thus the fossils may either be in the Twitya as historically described, or in the preglacial portion of the Ice Brook Formation (only the Stelfox Member of the Ice Brook is glacigenic). Geochemical measurements from left to right: (1) Highly reactive iron to total ratio (FeHR/FeT). Blue band represents values <0.38 and indicates potentially oxygenated conditions; values above 0.38 likely represent anoxic conditions. The dashed line at 0.2 is based on the lowest ratios seen in modern anoxic settings, and values below 0.2 are taken to reliably indicate oxic conditions (Table 1). (2) Iron in pyrite to highly reactive iron ratio (FeP/FeHR). For anoxic samples with FeHR/FeT >0.38, samples with ratios >0.8 are taken to indicate euxinic conditions, while lower values indicate ferruginous conditions. (3) Total iron to aluminum ratio (FeT/Al). Blue band represents average and standard deviation of oxic Paleozoic shale (Raiswell et al., 2008). (4) Molybdenum contents in ppm. Dashed vertical line represents average shale value (Turekian and Wedepohl, 1961). (5) Vanadium (ppm)/aluminum (wt%) ratio. Dashed vertical line represents average shale value of 16.25 (Turekian and Wedepohl, 1961); average upper continental crust (McLennan, 2001) is 13.0. (6) Pyrite $\delta^{34}S$ expressed in parts per mil (‰). Dashed line represents 0‰. (7) Weight percent total organic carbon (TOC). Abbreviations: Shez.—Shezal Formation, I.B.—Ice Brook Formation, Raven.—Ravensthroat formation, Sheep.—Sheepbed Formation. Lithologic log: s—shale, fs—fine sand, ms—medium sand, cs—coarse sand, cg—conglomerate. Coarser-grained samples from the Ice Brook Formation are marked as open circles.

is not exposed. The succeeding 66 m section of Twitya exposure consists of black shale that weathers with a yellow to orange oxidized rind. This is followed by another 63 m of predominantly dark-colored shale interbedded with thin siltstone beds. These strata coarsen upward to include fine- to medium-grained sandstone beds at 164 m, which is interbedded with shale and siltstone (60% shale and siltstone, 40% sandstone). Sedimentary structures are generally hard to discern due to cleavage, but some of the sandstones display normal grading, and slump folds are locally present. The interbedded shale, siltstone, and sandstone continue to 584 m in the cumulative measured section (Fig. 4).

At 584 m, a major change in sedimentary lithofacies occurs, marked by the appearance of quartz pebble- to granule-conglomerate channels, which regionally has been used to mark the base of the Ice Brook Formation (Aitken, 1991; Gordey et al., 2011). The succeeding 109 m section consists of channelized quartz pebble–granule-conglomerate interbedded with massive and convolute sandstone beds and thick-bedded sandstone beds with loading structures. The final 291 m section to the base of the Stelfox Member of the Ice Brook Forma-

tion consists of thin- to medium-bedded, fine- to medium-grained sandstone and siltstone with rare quartz pebble conglomerate. The sandstone beds have sharp bases, and some show normal-grading structures and slump folding. Although the finest-grained lithologies available were sampled for geochemistry, the samples from this interval are coarser (siltstone and fine-grained sandstone) than generally sampled for sedimentary geochemistry, and these are marked by open circles in Figure 4. Our section was measured on a ridgeline to provide continuous exposure, and although the original "Twitya disc" discovery site of Hofmann et al. (1990) in the valley below (note fossils were found in outcrop and scree over ~50 m of stratigraphy) cannot be traced precisely due to cover and lack of marker beds, the base of the discovery site is likely at ~710 m (estimate: ±20 m), in the lower Ice Brook Formation. Due to uncertainty about exact stratigraphic position and the definition of the Twitya and Ice Brook Formations through facies change in slope localities, we cannot be certain that the disks are not at a stratigraphic level correlative to the upper Twitya Formation as defined elsewhere, but it appears more likely that these should be assigned to the lower members of the Ice Brook Formation (slope equivalent of the Keele Formation; Aitken, 1991). Series of small-displacement (~5–10 m) normal faults cut the top of the section and may account for the slight thickness difference to the base of the Stelfox Member compared with Hofmann et al. (1990). No evidence of any wave-induced sedimentary structures was seen throughout the section, which, combined with the evidence for turbidites (graded bedding) and slump folding, suggests continuous deposition below storm wave base in a slope environment.

Sekwi Brook Stratigraphic Section

The stratigraphy and sedimentology of the Ediacaran succession at Sekwi Brook has been discussed in detail (Aitken, 1989; Dalrymple and Narbonne, 1996; MacNaughton et al., 2000; Macdonald et al., 2013; Narbonne et al., 2014). The succession begins above a Paleogene–Cretaceous thrust fault with black fissile shale and gray siltstone with slump structures that increase in prevalence up section. These strata are potentially correlative with the Sheepbed Formation sensu stricto (Macdonald et al., 2013). A >10-m-thick channelized conglomerate filled with quartz and lithic cobbles, medium- to coarse-grained sand, and redeposited giant ooids cuts down into the shale with up to 100 m of erosional relief. Based on lithostratigraphy, stratigraphic position, and carbon isotope chemostratigraphy, the shale, micrite, and fine-grained turbidite beds above this conglomerate represent the informally named June beds (Macdonald et al., 2013).

The June beds are succeeded by mixed carbonate-siliciclastic strata of the Gametrail and Blueflower Formation type sections (Aitken, 1989). The Gametrail Formation consists of 0–320 m of thin-bedded limestone interbedded with massive carbonate-clast debris flows and olistoliths. The first simple horizontal burrows occur in the basal Blueflower Formation (as defined by Aitken, 1989) in interbedded shale and micrite above a massive redeposited carbonate (Macdonald et al., 2013; Carbone and Narbonne, 2014). The Blueflower Formation consists of an informal lower member (~200 m thick) containing parallel-laminated and thin-bedded limestone and an upper member (~250 m thick) containing interbedded shale, siltstone, and thin-bedded sandstone. These thicknesses are approximate because even at their type locality, there are facies and thickness changes between closely measured sections (MacNaughton et al., 2000). Several channelized beds of conglomerate contain massive debrites composed of shallow-water carbonate (Aitken, 1989). The lower three quarters of the Blueflower Formation lack indicators of wave activity, which, combined with the presence of slumps throughout the section, again suggests deposition in a deep-water slope environment (MacNaughton et al., 2000). Near the top of the formation, the Blueflower shoals into medium-bedded hummocky cross-stratified sandstone and then abruptly into nearshore siliciclastic and carbonate facies and ultimately the paleokarst surface at the top of the Risky Formation.

Paleontology

Macroscopic fossils are common throughout the Cryogenian and Ediacaran succession of the Mackenzie Mountains. Cryogenian strata in the upper Twitya or lower Ice Brook Formation at Bluefish Creek contain abundant Twitya discs, i.e., impressions of centimeter-scale, soft-bodied, discoidal to hemispherical structures preserved on the soles of turbidite beds (Hofmann et al., 1990). As noted earlier, these probably occur in the nonglacial lower members of the Ice Brook Formation, but we refer to them as "Twitya discs" for historical continuity—the important point though is that they occur much closer to the end of the Cryogenian interglacial than the beginning (Fig. 4). Most discoidal specimens exhibit a sharp annulus (Fig. 2E), with some annulated discs also preserving a central tubercle and radial markings (Fig. 2F). Hemispherical forms are generally smooth, with some newly discovered specimens showing deformation features consistent with partial collapse of partly buried, hemispherical or spherical bodies, each with a tough but flexible outer membrane (Fig. 2G). Preservational comparisons can be drawn with the centimeter-scale hemispherical to discoidal fossil *Beltanelliformis* that dominates many shallow-water Ediacaran successions worldwide (Ivantsov et al., 2014). Twitya discs most likely represent soft-bodied creatures or colonies that were living on the Cryogenian seafloor at the time of arrival of the turbidite sands that preserved them, but their simple structure has thus far hindered accurate determination of their affinities.

Ediacaran strata at Sekwi Brook contain abundant impressions of soft-bodied Ediacara-type organisms (Hofmann, 1981; Narbonne and Aitken, 1990; Narbonne, 1994; Narbonne et al., 2014; Carbone et al., 2015). Ediacara-type impressions of fossil discs (*Aspidella*, *Hiemalora*, and *Eoporpita*) first appear on the bases of turbidite beds ~15 m above the base of the June beds and range throughout the unit. These discs are generally interpreted as the holdfasts of Ediacaran fronds, a view supported by the occurrence of stem impressions and even complete fronds (Fig. 2C) attached to some of these discs (Narbonne and Aitken, 1990; Narbonne et al., 2014). Contourites in the June beds contain rangeomorphs (*Fractofusus* [Fig. 2D], *Charnia*, and *Beothukis*) and an arboreomorph frond (*Charniodiscus*; Narbonne et al., 2014). All of these taxa are also known from the deep-water Mistaken Point assemblage (580–560 Ma) in Newfoundland (Narbonne et al., 2014; Liu et al., 2015).

Ediacara-type fossil impressions are absent from the coarsely crystalline carbonates of the overlying Gametrail Formation, but they occur sporadically throughout the Blueflower Formation. Simple discs are the most common, with rare occurrences of *Pteridinium* (Fig. 2B) and *Inkrylovia* in the deeper-water deposits that constitute the lower three quarters of the formation. Shoreface to offshore deposits at the top of the Blueflower Formation contain an assemblage of large discs, annulated tubes, and probable dickinsonids (Fig. 2A) that represent the youngest Ediacaran megafossils at Sekwi Brook and are similar to those found in late Ediacaran (560–541 Ma) shallow-water deposits worldwide (Carbone et al., 2015). The Blueflower Formation contains abundant small (~1-mm-diameter) burrows that completely cover bedding surfaces (Figs. 4A–4B) and probably represent microbial mat miners (Carbone and Narbonne, 2014). Larger (up to 1-cm-diameter) oblique burrows that represent the dwelling burrows of suspension feeders or

carnivores occur in the upper half of the Blueflower Formation (Figs. 3C–3D).

Sandy beds in the Risky Formation contain a few simple and oblique burrows similar to those of the underlying Blueflower Formation. Regionally, the Risky Formation is unconformably overlain by the Ingta Formation, which has been removed by erosion at Sekwi Brook but is present in the June Lake panel farther west. The upper half of the Ingta Formation contains complex trace fossils such as *Treptichnus*, *Plagiogmus*, and *Cruziana* (Carbone and Narbonne, 2014) and the small shelly fossil *Protohertzina* (Conway Morris and Fritz, 1980) diagnostic of an Early Cambrian age.

MATERIALS AND METHODS

Field and Laboratory Methods

In total, 165 samples, spanning up to 3 cm of stratigraphy, were collected from measured stratigraphic sections at Sekwi Brook and Bluefish Creek. All samples were appropriate for our geochemical techniques, specifically representing fine-grained lithologies including shale, calcareous shale, siltstone, and micrite. The exceptions to this are the seven coarser-grained samples from the Ice Brook Formation. Although sampling horizons may appear to be from coarser lithologies based on the stratigraphic sections in Figures 4 and 5, field samples were always collected from fine-grained horizons within these intervals. Regarding calcareous samples, Clarkson et al. (2014) recently investigated the applicability of the iron speciation proxy to carbonate-rich rocks and determined these techniques are appropriate for samples with >0.5 wt% total iron, a criterion surpassed by all of our samples. Each sample was trimmed of any weathered or altered material with a water-cooled rock saw and then crushed to flour in a shatterbox with a tungsten carbide container. Tungsten carbide grinding can impart contamination in cobalt, tungsten, and niobium, but it does not affect the elements

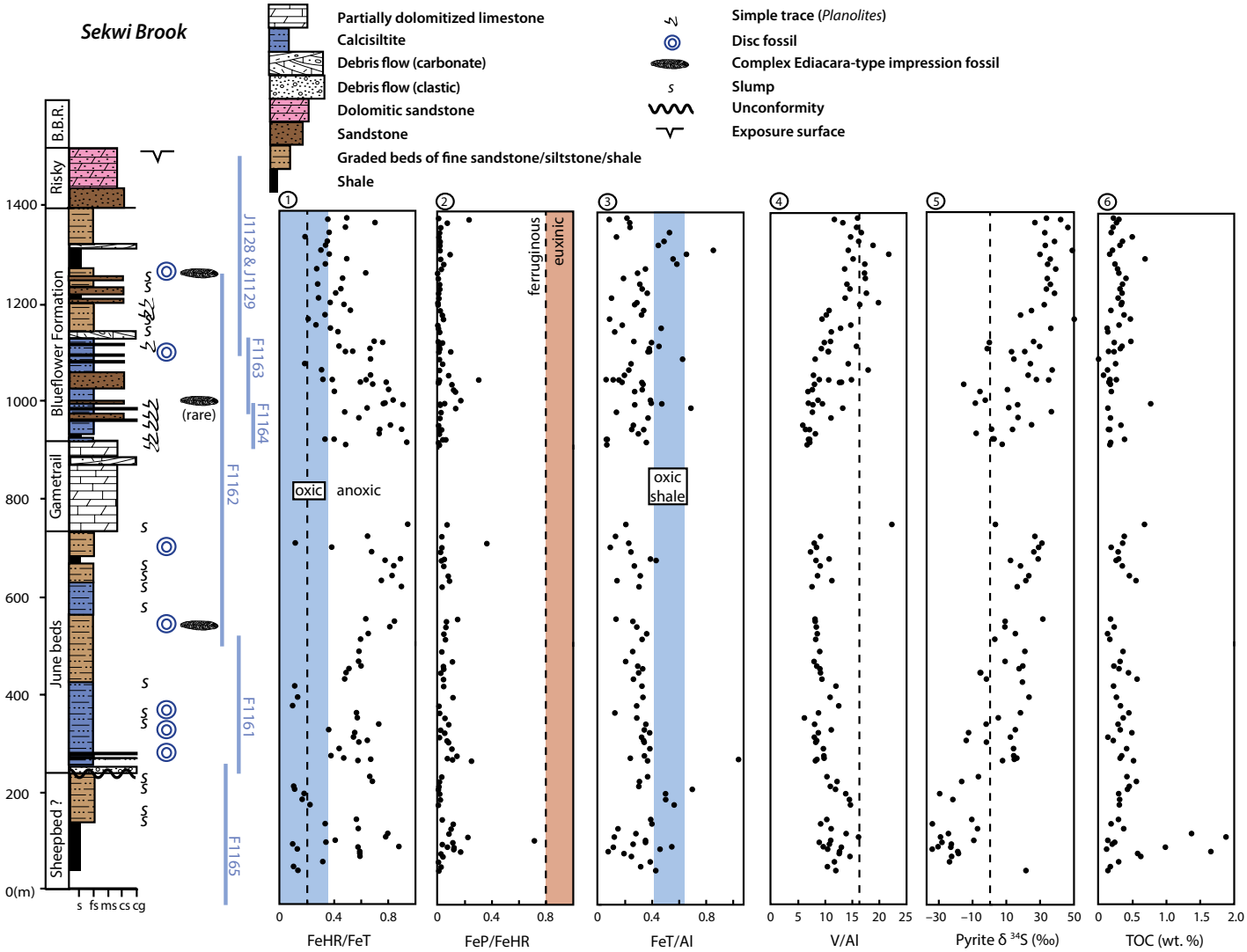

Figure 5. Multiproxy sedimentary geochemistry of the Sheepbed(?), June beds, Gametrail, and Blueflower formations, Sekwi Brook. Individual stratigraphic sections are shown as blue lines adjacent to stratigraphic column. Carbonate carbon isotope chemostratigraphy for this section can be found in Macdonald et al. (2013). Geochemical measurements from left to right (baseline values as in Fig. 4): (1) Highly reactive iron to total ratio (FeHR/FeT). (2) Iron in pyrite to highly reactive iron ratio (FeP/FeHR). (3) Total iron to aluminum ratio (FeT/Al). (4) Vanadium (ppm)/aluminum (wt%) ratio. (5) Pyrite $\delta^{34}S$ expressed in parts per mil (‰). (6) Weight percent total organic carbon (TOC). B.B.R.—Backbone Ranges Formation. Lithologic log: s—shale, fs—fine sand, ms—medium sand, cs—coarse sand, cg—conglomerate.

of interest here (Hickson and Juras, 1986; Rice et al., 2009). Total iron and quantification of the iron present as highly reactive phases—iron oxides, pyrite, iron carbonates, and magnetite—were reported in the supplementary compilation of Sperling et al. (2015) but are fully discussed here in the context of the stratigraphy and new trace-metal, pyrite sulfur isotope, and organic carbon data. Shale from the base of four fossiliferous (*Aspidella*) samples found in float was removed with a dental drill and analyzed for the aforementioned iron pools following Poulton and Canfield (2005). As discussed in that paper and in Sperling et al. (2015), precision for iron pools >0.3 wt% using these methodologies is better than 5% (percent standard error). Samples were then analyzed for the abundance of 32 additional elements, including redox-sensitive trace metals, using inductively coupled plasma–atomic emission spectrometry (ICP-AES) following standard four-acid digestion at SGS Laboratories, Canada. Pyrite sulfur isotope values were measured on silver sulfide obtained from a chromous chloride extraction (Canfield et al., 1986) via combustion in a Costech Elemental Analyzer linked to a Thermo Scientific Delta V mass spectrometer in continuous flow mode (measured as SO_2), and reported in standard delta notation relative to the value of Canyon Diablo troilite (VCDT). Long-term average standard deviations on standards when these samples were run were 0.23‰. Total inorganic carbon was quantified through mass loss upon acidification with 3 *N* HCl, and total organic carbon (TOC) was quantified by combusting acidified samples within a Carlo Erba NA 1500 Elemental Analyzer attached to a Thermo Scientific Delta V Advantage mass spectrometer. All geochemical results can be found in supplementary Table DR1.[1]

Interpretive Redox Framework

Iron-based proxies are one of the most mature and widely utilized lines of evidence for determining the redox character of water masses directly over accumulating sediments. Sediment deposited beneath anoxic water columns is enriched in both total (FeT) and highly reactive iron (FeHR, i.e., the iron in pyrite plus iron reactive toward biological and abiological reduction under anoxic conditions, specifically iron oxides, iron carbonates, and magnetite; Raiswell and Canfield, 1998; Lyons and Severmann, 2006; Poulton and Canfield, 2011). In modern basins, samples deposited beneath oxygenated water columns have ratios of highly reactive to total iron less than 0.38 (Raiswell and Canfield, 1998). Samples from beneath anoxic water columns generally have ratios greater than 0.38, although under rapid sedimentation rates—such as in the strata considered here—iron enrichments may be muted and result in a false "oxic" signature (Raiswell and Canfield, 1998). The magnitude of this effect can be estimated from modern sediments, and thus we use the lowest values of modern anoxic samples (from fig. 8 of Raiswell and Canfield, 1998) of 0.2 to differentiate unequivocally oxic from equivocal conditions in turbidite deposits (interpretive framework summarized in Table 1). We use the term "unequivocal" not in a general sense but only with respect to interpretations from this proxy. Iron speciation methods can also distinguish anoxic ferruginous water columns (with free ferrous iron) from euxinic water columns (with free sulfide) depending on the proportion of highly reactive iron present as pyrite (FeP), with FeP/FeHR ratios >0.8 taken to indicate a euxinic condition (Poulton and Canfield, 2011).

Data from total iron to aluminum ratios, pyrite sulfur isotopes, and redox-sensitive trace metals complement the iron speciation analyses and allow for deeper interrogation of redox patterns. FeT/Al ratios greater than the "average shale" value of 0.59 (Turekian and Wedepohl, 1961) or Paleozoic oxic average shale value of 0.53 ± 0.11 (Raiswell et al., 2008) generally indicate anoxic conditions. Redox-sensitive trace-metal enrichments above "average shale" values also indicate reducing conditions, especially when normalized to a biogeochemically conservative element such as aluminum. For the trace elements investigated here, notably molybdenum and vanadium, two caveats exist. First, during most of the Proterozoic, trace-metal enrichments in anoxic shales (as deduced from independent iron redox proxies) were low, which has been interpreted as a result of widespread reducing sinks (Reinhard et al., 2013). This impacts the utility of trace metals as a proxy because in contrast to classic Phanerozoic anoxic shales, subtle Proterozoic enrichments will be difficult to separate from background levels (Scott and Lyons, 2012). This is especially problematic given that Phanerozoic "average shale" values are not necessarily average oxic shales, but an unknown mixture of oxic (unenriched) and anoxic (enriched) shales—and the variance remains unpublished (discussed by Tribovillard et al., 2006). Second, the investigated sections are generally characterized by ferruginous conditions when anoxic (see Results). Molybdenum enrichments require the presence of sulfide to convert soluble molybdate to particle-reactive thiomolybdates (Helz et al., 1996), and vanadium enrichments under ferruginous conditions are not well studied. Thus, these elements provide a somewhat one-sided test: enrichments likely do indicate reducing conditions, but a lack of enrichment does not necessarily indicate oxygenated conditions (the difficulties of distinguishing oxic from ferruginous conditions is discussed by Sperling et al., 2014). Pyrite sulfur isotopes add complementary paleoenvironmental information by recording the isotopic offset between sulfide and coeval seawater sulfate records (reviewed for the Neoproterozoic Era by Halverson et al., 2010) as expressed during microbial sulfate reduction. Although there are myriad controls on fractionation (Sim et al., 2011; Leavitt et al., 2013; Gomes and Hurtgen, 2015; Bradley et al., 2015), large fractionations generally imply sulfate reduction in the presence of appreciable sulfate—either in the water column or in the shallow sediment but in diffusive contact with the overlying water column. In contrast, values similar to coeval sulfate generally indicate Rayleigh distillation either on a basinwide scale because of widespread sulfate reduction or within diffusion-limited sediment pore waters.

TABLE 1. INTERPRETATION SCHEME FOR IRON SPECIATION DATA ANALYZED FROM TURBIDITIC AND NONTURBIDITIC SETTINGS

FeHR/FeT	Depositional setting	Interpretation
>0.38	All	Anoxic
0.38–0.20	Turbiditic/rapid deposition	Equivocal
0.38–0.20	Nonturbiditic	Oxic
<0.20	All	Oxic

Note: FeHR—iron in pyrite plus iron reactive toward biological and abiological reduction under anoxic conditions, specifically iron oxides, iron carbonates, and magnetite; FeT—total iron. FeHR/FeT ratios >0.38 from most settings represent anoxic conditions (Raiswell and Canfield, 1998; Poulton and Canfield, 2011). In turbiditic settings (or under rapid deposition more broadly), highly reactive iron enrichments may be muted. The lowest ratio for anoxic turbiditic sediment is ~0.20 (Raiswell and Canfield, 1998), and turbiditic sediment with ratios beneath this value are considered to likely represent oxic conditions. The lowest ratio for modern anoxic turbidites is similar to, but not genetically related to, the Phanerozoic oxic average + standard deviation of 0.22 (Poulton and Raiswell, 2002), which is not applicable to the sequential extraction measurements in this study because it was generated using an older dithionite-only extraction protocol (Farrell et al., 2013). Interpretation of samples with ratios between 0.38 and 0.20 should be evaluated based on their sedimentological context.

[1]GSA Data Repository item 2015326, Table DR1, geochemical results (iron speciation values, elemental composition, pyrite sulfur isotope values, and total inorganic and organic carbon weight percentages), is available at http://www.geosociety.org/pubs/ft2015.htm or by request to editing@geosociety.org.

Trace Fossils

Trace-fossil specimens were collected from the Blueflower Formation during two field seasons at Sekwi Brook and were originally used to conduct a behavioral study analyzing the appearance of innovative feeding strategies as seen in the trace-fossil record (Carbone and Narbonne, 2014). All samples were collected from local float that could reasonably be traced back to its original outcrop area. Specimens on 129 trace-fossil–rich slabs from the earlier work were used in this study to investigate how burrow diameter varies with respect to stratigraphy and geochemistry. Many slabs are covered in multiple burrows (and multiple ichnogenera) that are observed to overlap and extend beyond the slab boundaries, making it impossible to distinguish the number of discrete burrows present on each slab. As a result, attempting to identify and measure all discrete traces per slab could provide biased results due to overcontribution by burrows that appear discrete but connect beyond the boundary of the slab. Additionally, the similarity of burrow diameters on any given slab makes it impossible to identify the number of individual trace makers. As a result, a weighting method was employed in order to quantify the number of burrows on each slab. This method is similar to the various semiquantitative visual estimation methods used by sedimentologists to estimate the amount of bioturbation in vertical or horizontal aspect (e.g., ichnofabric index; Droser and Bottjer, 1986). In order to determine the number of data points to count, each ichnogenus on each slab was assigned to one of five categories: one (~1–5 burrows), two (~6–10 burrows), three (~11–15 burrows), four (~15–20 burrows), five (~20+ burrows). Burrow diameters were measured (±0.1 mm), and the average burrow diameter of each ichnogenus on each slab was calculated. An ichnogenus with a weighting of one was given one data point in statistical analyses, whereas an ichnogenus with a weighting of five was given five data points in order to conservatively weight the abundance of each ichnogenus. This resulted in a total of 424 weighted burrow diameter data points, 272 from the lower Blueflower Formation and 152 from the upper Blueflower Formation.

The trace-fossil assemblage from the Blueflower Formation includes the first appearance of a variety of ichnogenera with different average burrow diameters (Carbone and Narbonne, 2014). As a result, the appearance of an individual ichnogenus has the capacity to affect the stratigraphic trend of burrow diameter. Therefore, burrow diameter analysis was also completed by isolating the ichnogenus *Helminthoidichnites*, a common trace fossil through the entire Blueflower Formation, in order to ascertain the change in burrow diameter within a single ichnogenus. In total, 80 slabs had *Helminthoidichnites* burrows, and 202 *Helminthoidichnites* weighted burrow diameter data points were used, 159 from the lower Blueflower Formation and 43 from the upper Blueflower Formation.

RESULTS

Bluefish Creek Sedimentary Geochemistry

Samples from interglacial strata at Bluefish Creek are characterized by two distinct geochemical states (Fig. 4; Table 2). The basal ~50 m of the Twitya Formation have FeHR/FeT ratios >0.38 and FeP/FeHR <0.80. The highly reactive iron pool is on average dominated almost exclusively by iron oxides (~90%) with trace amounts of the other three pools. There are modest enrichments in both molybdenum (5.4 ± 1.5 ppm; average and standard deviation) and vanadium (233 ± 34 ppm) compared to average shale compositions of 2.6 ppm and 130 ppm, respectively (Turekian and Wedepohl, 1961), and these enrichments remain if normalized to aluminum (Table 2). Total organic carbon contents are relatively high but not exceptionally so, between 0.57 and 1.85 wt%. Fe/Al

TABLE 2. GEOCHEMICAL CHARACTERISTICS OF THE BLUEFISH CREEK AND SEKWI BROOK SECTIONS

	% anoxic	% equivocal	% oxic	% ferruginous		
Bluefish Creek						
Basal ~50 m of Twitya	86	0	14	100		
Remaining Twitya + Ice Brook	0	36	64	N/A		
Sekwi Brook						
Sheepbed(?)	50	17	33	100		
June beds + lower Blueflower	84	9	7	100		
Upper Blueflower	47	53	3	100		
	FeP	Fe-dithionite	Fe-acetate	Fe-oxalate	FeT	FeHR
Bluefish Creek						
Basal ~50 m of Twitya	0.04 ± 0.05	0.94 ± 0.59	0.03 ± 0.02	0.03 ± 0.03	2.04 ± 0.79	1.04 ± 0.56
Remaining Twitya + Ice Brook	0.01 ± 0.02	0.60 ± 0.36	0.11 ± 0.09	0.05 ± 0.02	4.33 ± 1.54	0.74 ± 0.36
Sekwi Brook						
Sheepbed(?)	0.10 ± 0.21	0.78 ± 0.59	0.11 ± 0.08	0.04 ± 0.04	3.1 ± 1.38	1.02 ± 0.60
June beds + lower Blueflower	0.08 ± 0.08	1.32 ± 0.80	0.13 ± 0.12	0.03 ± 0.03	2.66 ± 1.13	1.56 ± 0.84
Upper Blueflower	0.03 ± 0.05	1.00 ± 0.53	0.08 ± 0.05	0.06 ± 0.05	2.88 ± 1.32	1.17 ± 0.60
	V (ppm)	V/Al	Mo (ppm)	Mo/Al	Fe/Al	Fe/Ti
Bluefish Creek						
Basal ~50 m of Twitya	233 ± 34	25.6 ± 4.0	5.4 ± 1.5	0.60 ± 0.18	0.22 ± 0.09	4.8 ± 2.5
Remaining Twitya + Ice Brook	156 ± 35	15.6 ± 2.0	2.1 ± 2.3	0.22 ± 0.23	0.45 ± 0.16	11.9 ± 5.1
Sekwi Brook						
Sheepbed(?)	109 ± 23	11.9 ± 1.9	1.2 ± 1.2	0.14 ± 0.16	0.34 ± 0.16	9.6 ± 4.9
June beds + lower Blueflower	90 ± 36	9.3 ± 2.7	0.9 ± 1.2	0.13 ± 0.13	0.30 ± 0.15	9.9 ± 5.6
Upper Blueflower	135 ± 34	14.7 ± 3.1	1.0 ± 1.1	0.13 ± 0.12	0.33 ± 0.18	8.6 ± 14.1
Average shale	130	16.25	2.6	0.33	0.53 ± 0.11*	10.26
Upper continental crust	107	13.31	1.5	0.19	0.44	8.54

Note: Top section: Percentage of samples likely to be anoxic, oxic, and equivocal based on iron speciation data as interpreted according to Table 1. Middle section: Iron pools from different extractions (Canfield et al., 1986; Poulton and Canfield, 2005) as average weight percent ± standard deviation. FeP—iron in pyrite from chromium reduction of sulfide extraction and stoichiometric calculation; Fe-dithionite—iron primarily in iron oxides such as hematite and goethite; Fe-acetate—iron in iron carbonates such as siderite and ankerite; Fe-oxalate—iron in magnetite; FeHR—iron in pyrite plus iron reactive toward biological and abiological reduction under anoxic conditions, specifically iron oxides, iron carbonates, and magnetite; FeT—total iron. Bottom section: Elemental abundances and ratios in relationship to average shale (Turekian and Wedepohl, 1961) and average upper continental crust (McLennan, 2001). Fe/Al average shale value and standard deviation (indicated by asterisk) is average normal shale of Raiswell et al. (2008); for reference, average shale of Turekian and Wedepohl (1961) is 0.59. The basal ~50 m of the Twitya Formation at Bluefish Creek includes the lowest seven samples through 71.9 m of stratigraphic height. At Sekwi Brook, Sheepbed(?) is equivalent to section F1165 on Figure 5, June beds + lower Blueflower Formation is equivalent to sections F1161, F1162, F1163, and F1164, and upper Blueflower Formation is equivalent to sections J1128 and J1129.

ratios are very low (0.22 ± 0.09), as are Fe/Ti ratios (4.79 ± 2.50), as compared to average shale. Pyrite sulfur isotopes are exceedingly heavy, beginning at ~35‰–40‰, becoming lighter down to 11‰, and then climbing back to values of 45‰ (note this positive trend occurs stratigraphically above the main inferred redox change in the section). Samples between 93 and 449 m did not have enough pyrite present for sulfur isotope measurements.

Samples above the basal ~50 m of the Twitya Formation are characterized by lower FeHR/FeT ratios (all below 0.38, and 64% of samples in the "unequivocal" oxic field below 0.2) and essentially no pyrite (0.01 ± 0.02 wt% iron in pyrite). Iron oxides remain the most abundant highly reactive phase on average (~80%). Fe/Al ratios are variable (0.45 ± 0.16) but generally within error of the oxic shale average. Molybdenum and vanadium contents are also generally at average shale values, although one sample has a Mo content of 14 ppm. TOC contents are relatively low (0.18 ± 0.11), and pyrite sulfur isotope values are variable (perhaps due to spotty stratigraphic coverage resulting from low sulfide yields) and range widely from –30‰ to 14‰.

Sekwi Brook Sedimentary Geochemistry

The Sekwi Brook section can be broken into three broad intervals with internally consistent geochemical signals (Fig. 5; Table 2). These intervals are defined by variation in iron speciation values and pyrite sulfur isotopes. In contrast, other metrics remain relatively constant throughout the composite section; for instance, the FeP/FeHR ratios of samples with anoxic iron speciation values are generally low (0.06 ± 0.09). The highly reactive iron pool is dominated by iron oxides (~80%), with subordinate pyrite, iron carbonates, and magnetite (Table 2). With respect to trace metals, Mo contents (not shown on Figure 5 due to lack of enrichments) and V contents are at or below average shale values (Table 2). Fe/Al ratios are depleted with respect to oxic shales (0.31 ± 0.16), while Fe/Ti ratios are closer to average shale (9.51 ± 8.49), albeit with high variability. TOC values are moderate (0.33 ± 0.27 wt%).

Shale at the base of the section (potentially correlative with the Sheepbed Formation) shows variable iron speciation signatures, with some samples falling in the unequivocally oxic zone (33%), some in the equivocal oxic zone (17%), and half in the anoxic region of calibrated FeHR/FeT space. While most anoxic samples have low FeP/FeHR ratios, one sample has a FeP/FeHR ratio of 0.71, which could be considered euxinic if some oxidative pyrite weathering of these field samples is taken into account (Poulton and Canfield, 2011). Pyrite sulfur isotopes are relatively low, around –10‰ to –30‰, and TOC values are bimodal, with generally low levels bracketing an interval with elevated contents (to ~2 wt%) between stratigraphic heights of 99 and 146 m.

The June beds and lower Blueflower Formation are characterized almost entirely by FeHR/FeT values >0.38. Specifically, 84% of samples from this interval fall in the anoxic field, and only 9% fall in the equivocal field and 7% in the oxic field. These values are consistent with six preliminary samples from the June beds at Sekwi Brook (listed as Sheepbed Middle Member) published in the compilation of Canfield et al. (2008), which had FeHR/FeT ratios between 0.73 and 0.86. Shale samples removed from the base of fossiliferous *Aspidella* samples from the June beds have ratios between 0.63 and 0.91 and no obvious differences in their geochemistry compared to other samples (Table 2; supplementary Table DR1 [see footnote 1]). Pyrite sulfur isotopes in the June beds are generally positive between 0‰ and 30‰, whereas those from the lower Blueflower are highly variable, between –16‰ and +27‰.

The upper Blueflower (as represented by sections J1128 and J1129) marks a shift to lower FeHR/FeT ratios. However, given the interpretive framework used here, the implications of this shift are uncertain, as the bulk of samples fall in the equivocal field (equivocal = 53%, anoxic = 47%, and oxic = 3%). V/Al ratios increase, as do some Fe/Al values, but only to roughly average shale values. Pyrite sulfur isotopes in this interval are exceptionally heavy, averaging 34.4‰ ± 7.8‰, and reaching up to 50‰.

Trace Fossils

Traces from the lower Blueflower Formation have a median and average diameter of 1.0 mm and 1.3 ± 0.6 mm, respectively; those from the upper Blueflower have a median and average of 1.5 mm and 2.1 ± 1.7 mm, respectively (Fig. 6). If only *Helminthoidichnites* burrows are considered, the lower Blueflower traces have a median of 1.0 mm and an average of 1.4 ± 0.5 mm, while the upper Blueflower traces have a median of 1.5 mm and an average of 1.9 ± 1.1 mm. To test for significant differences, the Wilcoxon rank sum test was used due to non-normal distributions (including after transformation). The lower and upper Blueflower trace diameters were found to be significantly different for all traces (chi square = 13.4, $p = 0.0003$). *Helminthoidichnites* burrows were not significantly different between the upper and lower Blueflower strata, but only slightly so according to traditional measures (e.g., $p < 0.05$) of significance (chi square = 3.7, $p = 0.054$); note also that *Helminthoidichnites* from the upper Blueflower are relatively rare (43 vs. 159 from lower Blueflower).

DISCUSSION

FeT/Al and FeHR/FeT Proxy Data

There is a clear discrepancy in evaluating the iron speciation signatures indicative of anoxic deposition (FeHR/FeT > 0.38) against Fe/Al values in these sections (Figs. 4 and 5). Specifically, sediments deposited beneath anoxic water columns should be enriched in total iron with respect to the background detrital load as estimated by Al contents (Lyons and Severmann, 2006), yet Fe/Al ratios from the basal 50 m of the Twitya Formation at Bluefish Creek (0.22 ± 0.09) and the entire Sekwi Brook section (0.31 ± 0.16) are well below the 0.59 average shale value of Turekian and Wedepohl (1961) or the 0.53 ± 0.11 average normal shale value of Raiswell et al. (2008). Several observations suggest that the inconsistency resides with the Fe/Al ratios rather than iron speciation data. First, the issue is not that the samples are simply unenriched and sit within the relatively narrow window of variation for oxic shales (Raiswell et al., 2008); rather, they are appreciably depleted in Fe with respect to Al—often more than two standard deviations of the mean from the oxic shale value. Iron ratios with respect to titanium (another biogeochemically conservative element often used to estimate background detrital input) remain depleted in the basal Twitya (Fe/Ti = 4.79 ± 2.50) but are closer to average shale in the Sekwi Brook section (Fe/Ti = 9.51 ± 8.49), albeit with extreme variance (average shale Fe/Ti = 10.26; Turekian and Wedepohl, 1961; Table 2). Overall, this speaks to differences in the Neoproterozoic iron and/or aluminum cycles that are currently poorly understood but will be an intriguing area of future research. While it is tempting to view this pattern as solely related to iron, since this element is depleted while aluminum is relatively normal, it is worth noting that the coefficient of determination (R^2) for aluminum-to-titanium is very low for the Sekwi Brook section ($R^2 = 0.16$; R^2 for Bluefish Creek = 0.56), potentially pointing to a different aluminum cycle as well. Because aluminum is biogeochemically inert, this would likely be related to provenance and/or weathering, although such a hypothesis would need to apply over a very large paleogeographic area to explain the pattern described here.

Intriguingly, high FeHR/FeT and low Fe/Al are beginning to emerge as a relatively common

pattern in Neoproterozoic basinal shales. For instance, this pattern is present in the ca. 800 Ma Fifteenmile Group of Yukon, Canada (Sperling et al., 2013), and roughly coeval Wynniatt Formation of Nunavut, Canada (Thomson et al., 2015), the Cryogenian Datangpo Formation, South China (Li et al., 2012), and the Ediacaran Doushantuo Formation, South China (Li et al., 2010). In these basins, many of the samples with high FeHR/FeT but very low Fe/Al are accompanied by redox-sensitive trace-metal abundances that suggest anoxic, if not also euxinic, depositional conditions. Based on these factors (especially the consistency with redox-sensitive trace metals), we consider the insights from iron speciation to be a more robust measure of basinal redox than Fe/Al ratios for these Neoproterozoic samples.

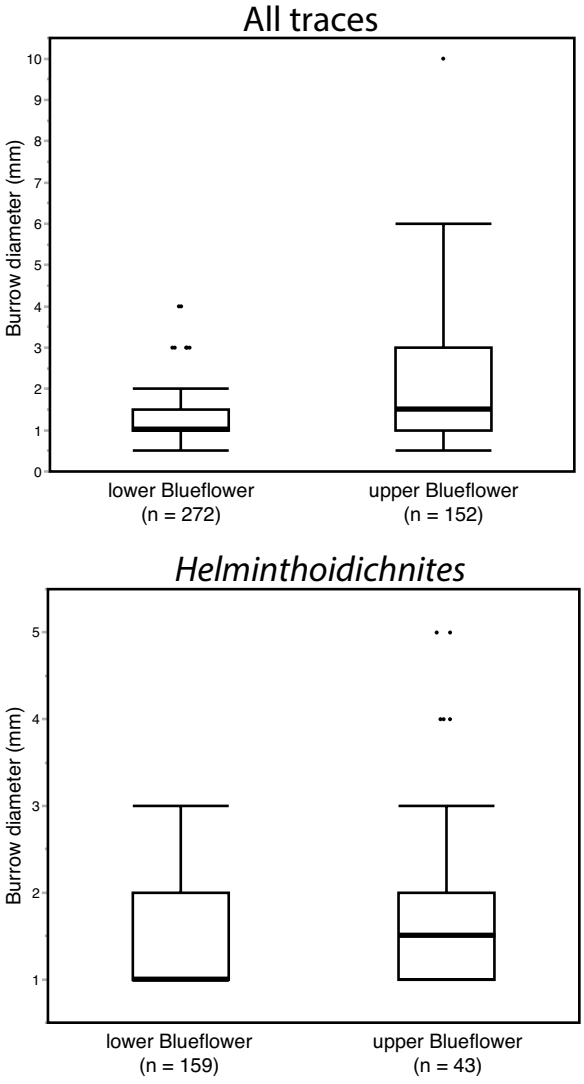

Figure 6. Standard boxplot analysis of trace-fossil diameters from the lower and upper Blueflower Formation. Solid black line represents median, box represents interquartile range spanning first to third quartiles, whiskers are at 1.5 times the interquartile range, and outliers above the whiskers are represented by open dots. (A) All burrows. (B) *Helminthoidichnites* burrows.

Redox State at Bluefish Creek

The lower ~50 m section of the Twitya Formation likely represents deposition under anoxic and ferruginous conditions and with very low seawater sulfate levels. This inference is supported by elevated FeHR/FeT ratios >0.38, low FeP/FeHR ratios <0.8, and low but present redox-sensitive trace-metal enrichments. We interpret elevated V levels in this interval in the conventional manner resulting from sequestration under an anoxic water column (Tribovillard et al., 2006), but we note the possibility exists for enrichment due to erosion of a mafic source such as the Franklin-age volcanics (Macdonald et al., 2010; Rooney et al., 2014). Extremely heavy pyrite sulfur isotopes captured in the lower Twitya Formation at Bluefish Creek are similar to those observed in Cryogenian nonglacial interlude strata in the Datangpo Formation, South China (Li et al., 2012), Tapley Hill and Aralka Formations, Australia (Gorjan et al., 2000; Hayes et al., 1992), Court Formation, Namibia (Gorjan et al., 2000), and in four samples lacking specific locality information from the Twitya Formation (Hayes et al., 1992). These high isotopic values are interpreted to result from drawdown of an initially very low oceanic sulfate pool by elevated levels of microbial sulfate reduction, resulting in residual heavy sulfate in deep waters through Rayleigh distillation (Li et al., 2012). Partial basinal restriction is hypothesized to exacerbate this process (Gomes and Hurtgen, 2015), which fits well with the inferred basin configuration of NW Canada at this time; however, the global distribution of these enriched pyrites speaks to a more fundamental feature of the Neoproterozoic ocean. Given the TOC abundances in these units, sulfate depletion during the Sturtian glacial episode and subsequent low seawater sulfate in the earliest Cryogenian appear to be the most reasonable conclusion.

This relatively short stratigraphic interval of anoxic conditions following the Sturtian glaciation was succeeded by generally oxygenated conditions for the remainder of the section. Essentially all records (FeHR/FeT, Mo, V) show a marked change to oxic (or average shale) values, which is mirrored by a decrease in TOC contents. This geochemical transition may be reflecting one of a number of scenarios. For instance, this redox change may reflect the time scale over which a reductant-rich ocean, adopted from the period of glaciation, is fully overturned and oxidized. Here, the time scale would be set by the mixing time of the ocean, and thus it would be on a 10^3 yr scale. This general scenario could be lengthened if one considers an episode of postglacial eutrophication, evidenced perhaps through the increase in TOC contents, which would provide an additional reductant flux for oxygenation to overcome. In total, this series of events would come at the net expense of oxidants (sulfate and O_2; more likely O_2 given the aforementioned sulfate argument). Whereas the dynamics of this scenario would fall under more local or basinal control, it is also possible that the change in redox proxy behavior is capturing a real change (increase) in background atmospheric pO_2. If such profound changes were to exist, there should exist a global and pronounced signature. Such a signature is lacking in studies of trace-metal contents in anoxic shales following the Sturtian glaciation (Li et al., 2012; Och and Shields-Zhou, 2012; Partin et al., 2013) and in a database analysis of Neoproterozoic iron speciation data (Sperling et al., 2015), suggesting that the oxygenation seen in the Bluefish Creek section may not represent a major event in the history of atmospheric O_2.

A growing wealth of redox data from across the Proterozoic now demonstrate that spatial

and geochemical heterogeneities abound. For instance, contemporaneous with the classic Mesoproterozoic example of sulfidic bottom-water conditions (Shen et al., 2003), there are examples of both oxygenated (Sperling et al., 2014) and ferruginous (Planavsky et al., 2011) conditions. In returning to the basin capturing the deposition of the Twitya and Ice Brook formations, we note that it is possible for more oxygenated conditions to have developed in this locality without the requirement of extensive global change. As the core target for this study is to better understand the relationship between early multicellular life and geochemistry, the key point is not the global redox landscape but the redox changes in this specific fossiliferous section. Since the majority of iron speciation points fall below the 0.2 ratio, clearly identifying oxic sediments in modern settings, we interpret these sediments as dominantly oxygenated. We do note however that some FeHR/FeT ratios fall in the "equivocal" zone for turbiditic sediments (Table 1), and a minority of samples have very slightly elevated Mo contents (4–14 ppm). It is also true that the coarse-grained samples (silt-to-fine sand) in the Ice Brook Formation that are in stratigraphic association with the fossils are not a calibrated lithology for iron speciation, although all samples (shale and siltstone) in the middle Twitya Formation that show the transition to oxygenated conditions are. In summary, any evidence for anoxia in the upper Twitya and Ice Brook Formations is circumstantial and/or stratigraphically limited.

Redox State at Sekwi Brook

Redox conditions at Sekwi Brook likely fluctuated between oxic and ferruginous throughout the depositional time frame of the upper group. While the potential Sheepbed correlative at the base shows a mixture of FeHR/FeT values <0.2 and >0.38, the June beds and lower Blueflower units are almost entirely dominated by FeHR/FeT ratios >0.38, with the exception of three oxic values at ~400 m (Fig. 5). The upper Blueflower Formation is marked by a shift to iron speciation ratios split between anoxic and equivocal water-column conditions. The very heavy pyrite sulfur isotope values in this late Ediacaran part of the section could again be a reflection of low seawater sulfate and part of a global pattern of heavy values in this interval (Gorjan et al., 2000).

In contrast to iron speciation data, Fe/Al ratios and redox-sensitive trace metals do not support anoxia. Caveats with both these proxies were discussed earlier, specifically, anomalous Fe/Al ratios across at least three basins during the Neoproterozoic and the lack of knowledge regarding trace-metal behavior under ferruginous conditions. A critical point in recognizing muted trace-metal enrichments is that "average shale" values (reviewed by McLennan, 2001) differ considerably between published studies (likely because of differential inclusion of both oxic and anoxic samples), and none gives a measure of variance. Average upper continental crust, which may be a better estimate for pure detrital input, has a lower vanadium content (107 ppm) than "average shale" (130 ppm; McLennan, 2001; Turekian and Wedepohl, 1961). In other words, some of the Sekwi samples do show slight enrichments with respect to this element, depending on the baseline value, but no notable enrichments.

Thus, the task becomes weighting the strengths of the various proxies. With respect to iron speciation, no applicable bias is known that would shift FeHR/FeT ratios from this depositional environment to such high values. Sediments deposited in very shallow-water settings (estuaries, salt marshes, and floodplains) can trap iron oxides, leading to FeHR enrichments and a false anoxic signature (Poulton and Raiswell, 2002). However, this bias is not relevant to these deep-water deposits. These rocks have experienced (subgreenschist) metamorphism, but the main effect of metamorphism is to convert highly reactive iron phases to poorly reactive chlorite or muscovite (Canfield et al., 2008; Raiswell et al., 2008). Based on the low Fe/Al ratios, it is unlikely these rocks have high levels of poorly reactive iron. More important, the effect is to lower FeHR/FeT ratios. The amount of carbonate present in some of the marly/micritic samples is also not to blame, as these samples have several weight percent total iron (Clarkson et al., 2014). As considerable caveats apply to the other redox proxies, especially the question of trace-metal enrichments (or lack thereof) in ferruginous conditions, and considering that all known biases would shift FeHR/FeT ratios to *lower* levels, we consider the iron speciation data to be the most robust indicator of paleo–redox conditions. Overall, the data from Sekwi Brook are therefore interpreted to indicate a dominantly ferruginous water column, congruent with iron speciation data published from the Goz A section in the Wernecke Mountains, which show the persistence of ferruginous conditions throughout the Ediacaran in NW Canada (Johnston et al., 2013).

Redox States Compared to the Body- and Trace-Fossil Record

The two investigated sections show different patterns with respect to redox changes and the appearance of body and trace fossils (Figs. 4 and 5). At Bluefish Creek, the change to apparent oxygenated conditions occurs low in the section, in the basal Twitya Formation, ~700 m below the appearance of the macroscopic discoidal fossils (Hofmann et al., 1990). In contrast, at Sekwi Brook, there is an almost anticorrelation between oxygenated conditions and the presence of fossils. The Sheepbed(?) Formation contains several intervals with oxygenated conditions (especially 205–243 m in section F1165) but no identified body fossils. The basal June beds contain *Aspidella* fossils and a clearly anoxic iron speciation signature; conversely, strata encompassing the three oxygenated points at 141–182 m in section F1161 are barren of fossils. Samples from sediments around the newly discovered biota of *Primocandelabrum*, *Namalia*, and rangeomorphs in the middle June beds (Narbonne et al., 2014) also show an anoxic signature, and these redox conditions persist through the first appearance of bilaterian traces in the Blueflower Formation.

The discovery of an oxygenated signal for the section bearing Cryogenian macroscopic discoidal fossils at Bluefish Creek is not surprising given that they were likely aerobic eukaryotes. However, an anoxic iron speciation signature throughout the Sekwi Brook section bearing Ediacaran fossils and bilaterian traces is unexpected and seemingly contradictory. Intermittent oxic conditions in shallow-water settings have been found in association with calcified Ediacaran metazoans (*Namacalathus* and *Cloudina*)—but not Ediacara-type impression fossils—in the Nama Group, Namibia (Wood et al., 2015; Darroch et al., 2015). In the modern ocean, fluctuating shallow-water redox conditions are not uncommon (Levin et al., 2009a), and various behavioral, metabolic, and molecular mechanisms allow organisms to deal with short-term hypoxia (Diaz and Rosenberg, 1995; Grieshaber et al., 1994; Grieshaber and Völkel, 1998). The Sekwi Brook fossils, present in a deep-water environment characterized by hundreds of meters of stratigraphically persistent anoxic iron speciation signature, require further explanation. One might first consider the possibility that these organisms are anaerobes. However, there are no known modern anaerobes of this size; the same fossil taxa (*Beothukis*, *Charnia*, *Charniodiscus*, *Fractofusus*, and *Primocandelabrum*) occur in aerobic strata at Mistaken Point (Canfield et al., 2007); and the bilaterian traces in the Blueflower Formation were undoubtedly made by obligate aerobes.

If both the iron speciation record of anoxia and the body/trace-fossil record requiring oxygen are robust, the most parsimonious reconciliation of the two data sets is through considering the different time scales of integration. The

geochemical samples collected here are fairly large and span 1–3 cm of stratigraphy. This sampling regime is common practice; for instance, a similar multiproxy geochemical study by Li et al. (2012) emphasized the collection of "large blocks (>200 g)." The geochemical fingerprint from a normal sample thus reflects an integration of the time scale over which those 1–3 cm of stratigraphy were deposited. Reasonably, 1–3 cm of shale will represent ~500–1500 yr, assuming modern average shale sedimentation rates (Einsele, 1992). This time scale is quite considerable from an ecological perspective. However, because many of the shales described here are associated with turbidites, they may represent less time, depending on whether they represent suspension fallout from a single flow (Bouma T_d) or background sedimentation (Bouma T_e). An additional consideration is that although geochemical sampling appears coincident with fossil appearances in Figure 5, this is in part a consequence of a 1500-m-thick stratigraphic column; many fossil samples are from local float, and even for in situ fossils, there was often a several-meter gap between the fossil occurrence and a suitable fine-grained lithology for geochemical measurement. Shales removed from the bottom of fossiliferous sandstone slabs are much more tightly linked temporally, and they are similar in geochemistry to the bulk samples (Tables 2 and 3). Importantly, these shale units represent the very tops (most condensed) of the T_e beds and therefore also represent a considerable (but unknown) amount of time. The point here is not to assign a specific amount of time to these beds, but to note our techniques are integrating geochemical signals over at least decadal if not centennial/millennial time scales.

In contrast, ecological recovery from hypoxic (low oxygen) and anoxic (no oxygen) conditions occurs on the time scale of several years or less (reviewed by Diaz and Rosenberg, 1995; Levin et al., 2009a). Faunal recovery generally begins with small, opportunistic meiofaunal and macrofaunal animals within days or weeks, and mature metazoan macrofaunal and megafaunal invertebrate communities are generally re-established within 2 yr. Communities in settings with predictable seasonal hypoxia/anoxia (especially those at the feather-edge of low O_2) may respond even faster—with the entire community changing composition and some organisms completely disappearing and reappearing over the course of the year (Santos and Simon, 1980; Levin et al., 2009b; Matabos et al., 2012). These communities are characterized by organisms with rapid growth, high dispersal potential, and developmental timing coordinated with oxygenation cycles.

TABLE 3. IRON GEOCHEMICAL DATA FROM SHALE REMOVED DIRECTLY FROM THE BASE OF SLABS BEARING *ASPIDELLA* SPECIMENS FROM SEKWI BROOK

Sample	FeT	Al	FeHR/FeT	FeP/FeHR	FeT/Al
N-89-115	1.79	10.1	0.91	0.13	0.18
N12-SB-4B	0.72	10.6	0.63	0.12	0.07
N91-21	3.27	7.66	0.89	0.16	0.43
N11-06-G4	2.6	7.13	0.74	0.02	0.36

Note: FeHR—iron in pyrite plus iron reactive toward biological and abiological reduction under anoxic conditions, specifically iron oxides, iron carbonates, and magnetite; FeT—total iron; FeP—iron in pyrite from chromium reduction of sulfide extraction and stoichiometric calculation.

These population-level features can then be compared to knowledge gained from other deep-water Ediacaran communities such as at Mistaken Point, Newfoundland (reviewed by Liu et al., 2015). Population structure data from that locality are interpreted as indicating that rangeomorph populations reproduced continuously and had at least some variety of larval dispersal mechanism (Darroch et al., 2013). Given this model, stable Ediacaran communities living in more-oxygenated environments in NW Canada or elsewhere would have produced a continuous pool of recruits capable of rapidly colonizing the Sekwi Brook seafloor. These communities would have grown and briefly flourished on very short ecological time scales before being locally extirpated by the return of anoxic conditions. The small bilaterian trace makers in the lower Blueflower Formation also easily fit such a model, as far larger burrowing bilaterians are capable of rapidly recolonizing areas after a subtle increase in oxygen levels (Levin et al., 2009b).

We view this scenario, one of differing characteristic time scales, as the most likely reconciliation between the geochemical and paleontological data at Sekwi Brook. Unfortunately, it remains difficult to explicitly test given the current sharpness of our geochemical toolkit, the time resolution of sedimentary proxies, and the nature of the stratigraphic and paleontological records. Fortunately, there are Phanerozoic analogs to this dilemma. There are numerous instances in the geochemical record where apparently rapid fluctuations in oxygen levels—not recognizable in the integrated geochemical record—have controlled colonization on ecological time scales. For instance, the Upper Cambrian Alum Shale of Sweden contains intervals with sub-millimeter-scale burrows and rare benthic trilobites (Clarkson et al., 1998), as well as clear iron and molybdenum geochemical evidence for overall persistent euxinia (Gill et al., 2011). A similar pattern, from a variety of proxy evidence, can be seen in the Jurassic Kimmeridge Clay (Raiswell et al., 2001) and Oxford Clay (Kenig et al., 2004) of the United Kingdom, the Devonian Upper Kellwasser horizon in New York State (Boyer et al., 2014), and in Cretaceous sediments from the Demerara Rise, equatorial Atlantic Ocean (Jimenez Berrocoso et al., 2008). The simplest resolution of these disparate observations is that transient oxygenations are likely a common feature of "homogeneous" anoxic black shale (Schieber, 2003). Interestingly, the opposite is also true; microstratigraphic analyses of two sections in the Devonian Hamilton Group, New York, demonstrated several 5–10 cm intervals that were devoid of body and trace fossils but still showed a dominantly oxic (albeit potentially dysoxic) geochemical signal (Boyer et al., 2011). In this case, sediment outside the barren zones contained a stressed, dysaerobic fauna likely on the edge of their oxygen tolerance. The barren intervals then represent either a further decrease in oxygen (technically still oxic but below the O_2 requirements of the organisms) or an increased frequency of extremely transient anoxic events. Either of these might exclude animals while still preserving an "oxic" geochemical signature.

The possibility must remain open that the Sekwi Brook section and the examples cited here represent an exceptional failure of multiproxy geochemical interrogation; however, all are interpreted by the respective authors as representing a temporal disconnect between geochemical and ecological time scales. Continued coupling of microstratigraphic biotic and geochemical studies (e.g., Boyer et al., 2011; Farrell et al., 2013) and modeling of integration time scales will provide welcome insight into the limits of temporal resolution possible in the geochemical record. It will further define our capacity to, in fine structure, speak to the tolerance and controls of local environments on incipient and colonizing fauna in the geological record. In sum, and as it relates to Ediacaran observations, the organisms at Sekwi Brook clearly required oxygenation on ecological time scales, but the geochemical data refute the hypothesis that a stable oxygenated condition in this or any other basin was required for the appearance of these Avalon-assemblage Ediacaran organisms (Fig. 7). Whether stable oxygenation was required for the appearance of more muscular and mobile bilaterians (Johnston et al., 2012) such as *Kimberella*—presumably with higher O_2 demand—will need further study.

Although geologically stable oxygenation is not required for the appearance of these

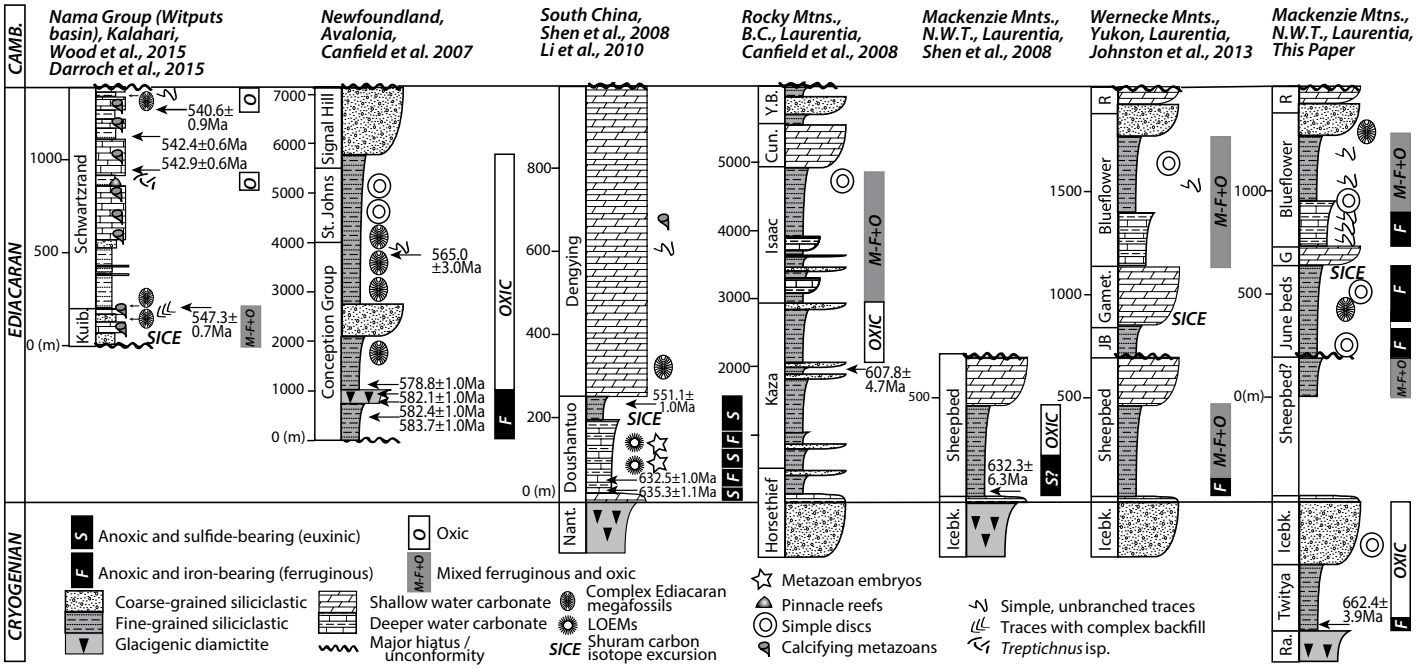

Figure 7. Relationship between redox state and the appearance of megascopic fossils at investigated Ediacaran sections worldwide. Redox change may correspond to the appearance of megascopic fossils in some sections, but stable oxygenation on geologic time scales is not required. Sources of the redox data are shown on figure. Physical stratigraphy, biostratigraphy, and chronostratigraphy are adapted from Macdonald et al. (2014); Kalahari is modified after Grotzinger et al. (1995); Newfoundland is modified after Liu et al. (2010); South China is modified after Zhou and Xiao (2007) and Condon et al. (2005); Rocky Mountains data of British Columbia are modified after Ross et al. (1995); Mackenzie and Wernecke Mountains of the Northwest Territories and Yukon are after Macdonald et al. (2013) and Rooney et al. (2015). Ages were recalculated by Schmitz (2012). LOEMs—Large Ornamented Ediacaran Microfossils; CAMB.—Cambrian; Kuib.—Kuibis; Nant.—Nantuo; Horsethief—short for Horsethief Creek; Cun.—Cunningham; Y.B.—Yankee Belle; Icebk.—Ice Brook; J.B.—June beds; Gamet. and G—Gametrail; R—Risky; Ra.—Rapitan; N.W.T.—Northwest Territories; B.C.—British Columbia. Question marks in interpretation of data from Shen et al. (2008) are because that study used an older dithionite-only extraction methodology that is less useful for distinguishing euxinic from ferruginous conditions.

Ediacara-type organisms or simple bilaterian traces, it may have played a role in organismal abundance and burrow size. The June beds and Blueflower body fossil biotas are moderately diverse, but the fossils are relatively rare (most species are represented by a single specimen) compared to similarly aged biotas in Newfoundland or England (Liu et al., 2015). This may be an entirely taphonomic control, but it may also reflect a stressed community living on the very edge of its oxygen tolerance. With respect to burrow diameter, we note that between the lower and upper Blueflower units, there is a shift from mainly anoxic to mixed anoxic and equivocal iron speciation values (Fig. 5). The proportion of samples with FeHR/FeT ratios above and below 0.38 in the lower and upper Blueflower units is statistically significant (Pearson chi-square test; chi square = 8.4, $p = 0.0037$). This shift correlates with the significant increase in trace-fossil burrow diameter (Fig. 6). While it is tempting to infer causality, this must be tempered somewhat because these FeHR/FeT ratios between 0.38 and 0.2 could represent muted enrichments during rapid deposition. Nonetheless, this shift (if it indeed represents oxygenation) provides the best evidence in the Sekwi Brook section for changing oxygen levels affecting eukaryotic life in the Ediacaran oceans of NW Canada.

Facies Controls on the Appearance of the Ediacaran Biota in NW Canada

If persistent or long-lived oxygenation was not controlling the stratigraphic appearance of macroscopic fossils at Sekwi Brook and Bluefish Creek—what was? The most obvious explanation is simply the distribution of beds capable of preserving fossils. Certainly, there are a number of distinct sedimentological, geochemical, and microbiological factors involved in the preservation of Ediacaran fossils (Gehling, 1999; Callow and Brasier, 2009; Darroch et al., 2012), but the distinction drawn here is even more basic. Many of the strata in the Windermere Supergroup would not, for various reasons, be expected to preserve any fossils whatsoever—exceptional or otherwise (Fig. 8). For instance, at Bluefish Creek, the Shezal Formation diamictite would obviously not preserve fossils, and most of the Twitya Formation consists of relatively homogeneous, cleaved, thin-bedded, and fine-grained strata. In other words, most of the Twitya Formation does not contain the type of well-defined bedding soles on which macroscopic fossils are generally preserved in the Windermere Supergroup (Hofmann et al., 1990; Narbonne and Aitken, 1990; Narbonne et al., 2014). The base of the Ice Brook Formation as mapped here (Gordey et al., 2011) consists of quartz-pebble conglomerate channels and massive to slumped sandstone units, again with low preservational potential. The appearance of the macroscopic discoidal fossils corresponds with the appearance of abundant, stratified turbidites with well-defined bases (Fig. 7).

At Sekwi Brook, the exposed section of the putative Sheepbed Formation shows no macroscopic fossils, even though it contains more of a mixed oxic-ferruginous signature than the overlying June beds. Field investigation of these strata revealed the reason: Like the basal

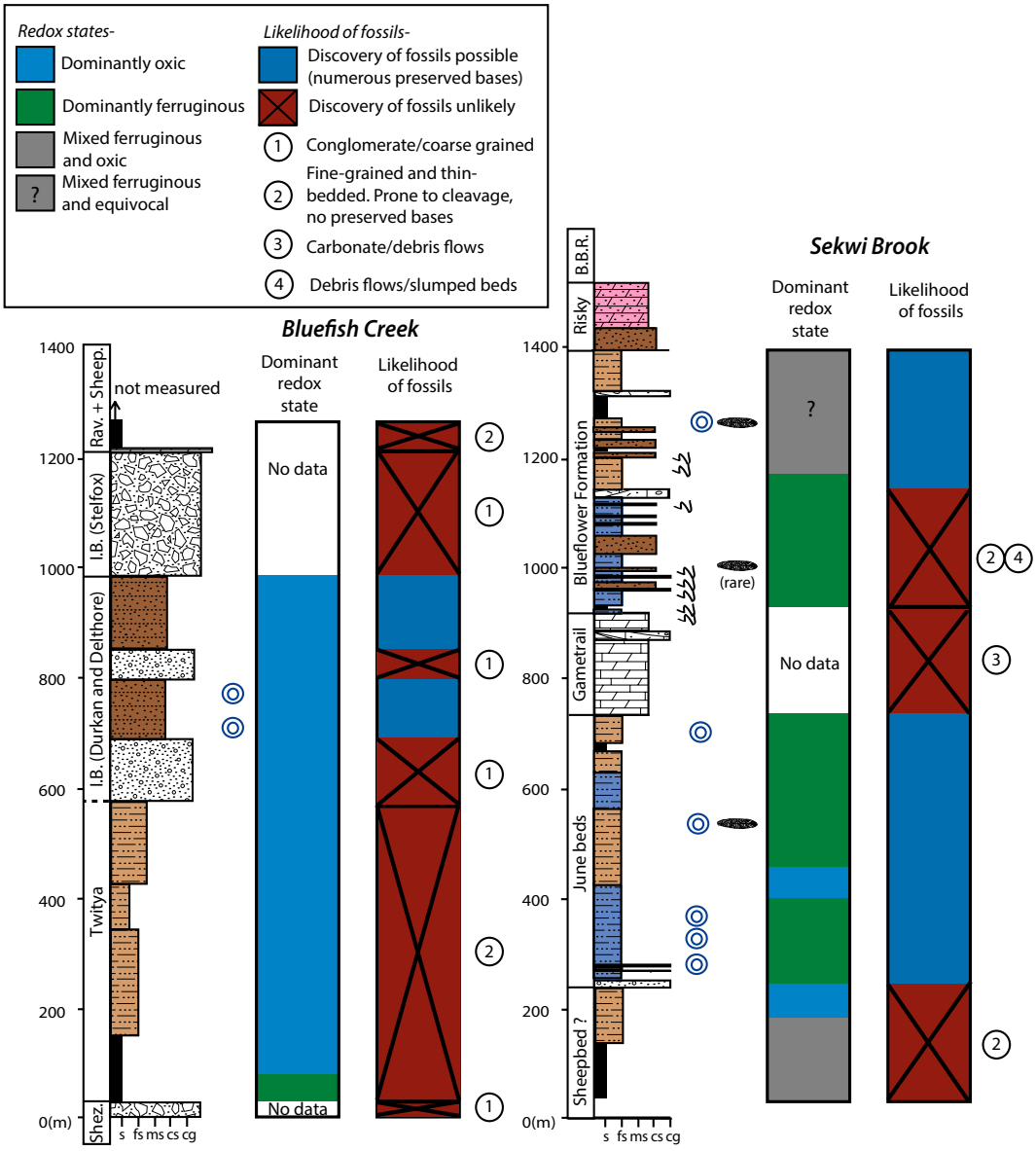

Figure 8. Comparison of redox and preservational controls on the stratigraphic distribution of macrofossils at Bluefish Creek and Sekwi Brook. Abbreviations: Shez.—Shezal Formation, I.B.—Ice Brook Formation, Rav.—Ravensthroat formation, Sheep.—Sheepbed Formation; B.B.R.—Backbone Ranges Formation. Lithologic log: s—shale, fs—fine sand, ms—medium sand, cs—coarse sand, cg—conglomerate.

Twitya, these shale- and siltstone-dominated units contain a penetrative cleavage and tend to separate on cleavage planes rather than bedding surfaces. Crossing the unconformity into the basal June beds, the first beds with well-defined bases appear, and with them the first *Aspidella* discoidal fossils. In fact, the strata containing many of the most remarkable fossils described to date (*Primocandelabrum* and *Namalia*; Narbonne et al., 2014) are characterized by a heterolithic mixture of erodible shale/micrite and more resistant beds with defined bases (rangeomorphs and arboreomorphs from the same strata are preserved as intrastratal features within contourite beds; Figs. 3A–3D; Narbonne et al., 2014). The case for a facies control on fossil preservation in the Blueflower Formation is less clear. Much of the lower Blueflower Formation is dominated by mixed carbonate and shale without well-defined soles to beds and without Ediacaran fossils. Nonetheless, abundant bilaterian trace fossils are present on thin, often millimeter-thick beds (Hofmann, 1981; Carbone and Narbonne, 2014). These beds are far thinner than those typically hosting Ediacaran mold-style preservation, but aside from this bed thickness difference, there is no apparent large-scale taphonomic control. The upper Blueflower Formation contains mixed sandstone, siltstone, and shale, with well-defined soles of beds and spectacular Ediacara-style fossil preservation (Narbonne, 1994; Carbone et al., 2015).

The strongest control on the appearance of macroscopic Neoproterozoic fossils in NW Canada may then be quite prosaic. Without the appropriate facies for preservation, and, in particular, the presence of well-defined bedding soles in a heterolithic succession, which are required to form the sizable fossiliferous slabs Ediacaran paleontologists seek, there are no fossils. Thus, the appearance of fossils in a given stratigraphic succession can be thought of in terms of environmental and presentation factors. It is recognized there may also be genetic factors at play (e.g., Erwin et al., 2011) and that oxygen is only a component of a permissive environment—food availability, ecological interactions, and other abiotic factors such as temperature play equally important roles. Much of the discussion on the origins of Ediacara-type organisms, however, has focused on oxygen (e.g., Canfield et al., 2007; Shen et al., 2008), and given the methodological similarity of our study, we retain that focus. With regards

to oxygen, such as can be measured, the environmental requirements at Bluefish Creek were met well before the preservational factors were satisfied, namely, beds with defined soles suitable for preserving fossils. At Sekwi Brook, the environmental requirements for oxygen may have been met only briefly on a time scale of years to decades, but fossils could not be presented until the June beds. In each case, it is not possible to directly compare oxygenation trends with fossil first appearances because the correct taphonomic control does not exist.

This has implications in considering the possible stratigraphic range of the Ediacaran biota. These organisms are generally considered to have evolved in the mid- to late Ediacaran (Xiao and Laflamme, 2009; Narbonne et al., 2012), and indeed the first June bed fossils are likely <580 Ma (Macdonald et al., 2013). Nonetheless, in regions such as the Mackenzie Mountains, they cannot be conclusively excluded from the basal Ediacaran because appropriate beds for preservation and presentation do not exist. Consequently, sustaining global hypotheses for a mid-Ediacaran origin for the Ediacara biota or hypotheses relating environmental change to their origin should take place in a stratigraphic framework considering varying likelihoods of preservation (Patzkowsky and Holland, 2012).

CONCLUSIONS

The abrupt appearance of macroscopic fossils in the later Neoproterozoic has been related to different driving mechanisms, and the exceptionally well-developed stratigraphic record of NW Canada provides an excellent laboratory in which to continue unraveling these causal factors. In the investigated Cryogenian Bluefish Creek section and Ediacaran Sekwi Brook section, oxygenation is not well correlated with the appearance of fossils. At Bluefish Creek, the appearance of oxygenated conditions occurs low in the Twitya Formation, hundreds of meters stratigraphically below the appearance of macroscopic discoidal fossils. At Sekwi Brook, iron speciation data imply that anoxic and ferruginous conditions continued throughout the appearance of Ediacaran fossils and the first simple bilaterian trace fossils. This implies that the organisms were likely transiently colonizing the seafloor at Sekwi Brook during brief oxygenation events not recorded in bulk geochemical measurements. This relationship between the fossils and geochemistry is at apparent odds with the absolute oxygen requirements of these organisms, but this is seen in many Phanerozoic black shales due to the different time scales integrated by ecological and geochemical data. Importantly, these data suggest that stable oxygenation of a basin is not required for the appearance of many Ediacaran taxa. To a first-order approximation, more so than oxygenation, the appearance of fossils of large eukaryotes throughout the entire Cryogenian and Ediacaran succession in NW Canada is dictated almost entirely by the appearance of event beds suitable for their preservation and presentation.

ACKNOWLEDGMENTS

We thank Weiquan Mai, Alex Morgan, Austin Miller, Erin Beirne, and Andy Masterson for help in the laboratory, Alan Rooney, Caitlin Rush, Ally Brown, and Thomas Boag for assistance in the field, Ben Gill, Marcus Kunzmann, Simon Darroch, and Marc Laflamme for helpful discussion, Dugald Dunlop from Meridian Mining via Colorado Minerals for logistical help, and Canadian and Fireweed Helicopters for safe and reliable transportation. Sperling was supported by postdoctoral fellowships from the Agouron Institute, National Aeronautics and Space Administration Astrobiology Institute (NAI), and National Science Foundation (NSF) EAR-1324095 over the course of this project. Geochemical analyses were supported by NSF EAR-1324095 (to Sperling and Johnston). Johnston and Macdonald were supported by the Massachusetts Institute of Technology node of the NAI. Macdonald recognizes NSF SGP EAR-1148058 for additional support. Narbonne acknowledges funding through a Natural Sciences and Engineering Research Council of Canada Discovery Grant and a Queen's Research Chair.

REFERENCES CITED

Aitken, J.D., 1989, Uppermost Proterozoic Formations in Central Mackenzie Mountains, Northwest Territories Geological Survey of Canada Bulletin 368, 26 p.

Aitken, J.D., 1991, The Ice Brook Formation and Post-Rapitan, Late Proterozoic Glaciation, Mackenzie Mountains, Northwest Territories: Geological Survey of Canada Bulletin 404, 43 p.

Bond, G.C., Christie-Blick, N., Kominz, M.A., and Devlin, W.J., 1985, An Early Cambrian rift to post-rift transition in the Cordillera of western North America: Nature, v. 315, p. 742–746, doi:10.1038/315742a0.

Boyer, D.L., Owens, J.D., Lyons, T.W., and Droser, M.L., 2011, Joining forces: Combined biological and geochemical proxies reveal a complex but refined high-resolution palaeo-oxygen history in Devonian epeiric seas: Palaeogeography, Palaeoclimatology, Palaeoecology, v. 306, p. 134–146, doi:10.1016/j.palaeo.2011.04.012.

Boyer, D.L., Haddad, E.E., and Seeger, E.S., 2014, The last gasp: Trace fossils track deoxygenation leading into the Frasnian-Fammenian extinction event: Palaios, v. 29, p. 646–651, doi:10.2110/palo.2014.049.

Bradley, A.S., Leavitt, W.D., Schmidt, M., Knoll, A.H., Girguis, P.R., and Johnston, D.T., 2015, Patterns of sulfur isotope fractionation during microbial sulfate reduction: Geobiology, doi:10.1111/gbi.12149 (in press).

Callow, R.H.T., and Brasier, M.D., 2009, Remarkable preservation of microbial mats in Neoproterozoic siliciclastic settings: Implications for Ediacaran taphonomic models: Earth-Science Reviews, v. 96, p. 207–219, doi:10.1016/j.earscirev.2009.07.002.

Canfield, D.E., Raiswell, R., Westrich, J.T., Reaves, C.M., and Berner, R.A., 1986, The use of chromium reduction in the analysis of reduced inorganic sulfur in sediments and shale: Chemical Geology, v. 54, p. 149–155, doi:10.1016/0009-2541(86)90078-1.

Canfield, D.E., Poulton, S.W., and Narbonne, G.M., 2007, Late-Neoproterozoic deep-ocean oxygenation and the rise of animal life: Science, v. 315, p. 92–95, doi:10.1126/science.1135013.

Canfield, D.E., Poulton, S.W., Knoll, A.H., Narbonne, G.M., Ross, G., Goldberg, T., and Strauss, H., 2008, Ferruginous conditions dominated later Neoproterozoic deep-water chemistry: Science, v. 321, p. 949–952, doi:10.1126/science.1154499.

Carbone, C., and Narbonne, G.M., 2014, When life got smart: The evolution of behavioral complexity through the Ediacaran and Early Cambrian of NW Canada: Journal of Paleontology, v. 88, p. 309–330, doi:10.1666/13-066.

Carbone, C., Narbonne, G.M., Macdonald, F.A., and Boag, T., 2015, New Ediacaran fossils from the uppermost Blueflower Formation, NW Canada: Disentangling biostratigraphy and paleoecology: Journal of Paleontology, v. 89, p. 281–291, doi:10.1017/jpa.2014.25.

Clarkson, E.N.K., Ahlberg, P., and Taylor, C.M., 1998, Faunal dynamics and microevolutionary investigations in the upper Cambrian Olenus zone at Andrarum, Skane, Sweden: GFF, v. 120, p. 257–267, doi:10.1080/11035899809453214.

Clarkson, M.O., Poulton, S.W., Guilbaud, R., and Wood, R.A., 2014, Assessing the utility of Fe/Al and Fe-speciation to record water column redox conditions in carbonate-rich sediments: Chemical Geology, v. 382, p. 111–122, doi:10.1016/j.chemgeo.2014.05.031.

Colpron, M., Logan, J.M., and Mortensen, J.K., 2002, U-Pb zircon age constraint for late Neoproterozoic rifting and initiation of the Lower Paleozoic passive margin of western Laurentia: Canadian Journal of Earth Sciences, v. 39, p. 133–143, doi:10.1139/e01-069.

Condon, D.J., Zhu, M., Bowring, S.A., Wang, W., Yang, A., and Jin, Y., 2005, U-Pb ages from the Neoproterozoic Doushantuo Formation, China: Science, v. 308, p. 95–98, doi:10.1126/science.1107765.

Conway Morris, S., and Fritz, W.H., 1980, Shelly microfossils near the Precambrian-Cambrian boundary, Mackenzie Mountains, northwestern Canada: Nature, v. 286, p. 381–384, doi:10.1038/286381a0.

Dalrymple, R.W., and Narbonne, G.M., 1996, Continental slope sedimentation in the Sheepbed Formation (Neoproterozoic, Windermere Supergroup), Mackenzie Mountains, N.W.T.: Canadian Journal of Earth Sciences, v. 33, p. 848–862, doi:10.1139/e96-064.

Darroch, S.A.F., Laflamme, M., Schiffbauer, J., and Briggs, D.E.G., 2012, Experimental formation of a microbial death mask: Palaios, v. 27, p. 293–303, doi:10.2110/palo.2011.p11-059r.

Darroch, S.A.F., Laflamme, M., and Clapham, M.E., 2013, Population structure of the oldest known macroscopic communities from Mistaken Point, Newfoundland: Paleobiology, v. 39, p. 591–608, doi:10.1666/12051.

Darroch, S.A.F., Sperling, E.A., Boag, T.H., Racicot, R.A., Mason, S.J., Morgan, A.S. Tweedt, S., Myrow, P., Johnston, D.T., Erwin, D.H., Laflamme, M., 2015, Biotic replacement and mass extinction of the Ediacaran biota: Proceedings of the Royal Society Series B, v. 282, doi:10.1098/rspb.2015.1003.

Devlin, W.J., 1989, Stratigraphy and sedimentology of the Hamill Group in the northern Selkirk Mountains, British Columbia: Evidence for latest Proterozoic–Early Cambrian extensional tectonism: Canadian Journal of Earth Sciences, v. 26, p. 515–533, doi:10.1139/e89-044.

Devlin, W.J., and Bond, G.C., 1988, The initiation of the early Paleozoic Cordilleran miogeocline: Evidence from the uppermost Proterozoic–Lower Cambrian Hamill Group of southeastern British Columbia: Canadian Journal of Earth Sciences, v. 25, p. 1–19, doi:10.1139/e88-001.

Diaz, R.J., and Rosenberg, R., 1995, Marine benthic hypoxia: A review of its ecological effects and the behavioral responses of benthic macrofauna: Oceanography and Marine Biology, v. 33, Annual Review, p. 245–303.

Droser, M.L., and Bottjer, D.J., 1986, A semiquantitative field classification of ichnofabric: Journal of Sedimentary Research, v. 56, p. 558–559, doi:10.1306/212F89C2-2B24-11D7-8648000102C1865D.

Droser, M.L., Gehling, J.G., and Jensen, S., 1999, When the worm turned: Concordance of Early Cambrian ichnofabric and trace-fossil record in siliciclastic rocks of South Australia: Geology, v. 27, p. 625–628, doi:10.1130/0091-7613(1999)027<0625:WTWTCO>2.3.CO;2.

Einsele, G., 1992, Sedimentary Basins: Evolution, Facies, and Sediment Budget: Berlin, Springer-Verlag, 628 p.

Eisbacher, G.H., 1981, Sedimentary tectonics and glacial record in the Windermere Supergroup, Mackenzie Mountains, northwestern Canada: Geological Survey of Canada Paper 80–27, 40 p.

Erwin, D.H., and Valentine, J.W., 2013, The Cambrian Explosion: Greenwood Village, Colorado, Roberts and Company Publishers, 416 p.

Erwin, D.H., Laflamme, M., Tweedt, S.M., Sperling, E.A., Pisani, D., and Peterson, K.J., 2011, The Cambrian conundrum: Early divergence and later ecological success in the early history of animals: Science, v. 334, p. 1091–1097, doi:10.1126/science.1206375.

Farrell, U.C., Briggs, D.E.G., Hammarlund, E.U., Sperling, E.A., and Gaines, R.R., 2013, Paleoredox and pyritization of soft-bodied fossils in the Ordovician Frankfort Shale of New York: American Journal of Science, v. 313, p. 452–489, doi:10.2475/05.2013.02.

Fritz, W.H., 1982, Vampire Formation, a New Upper Precambrian (?)/Lower Cambrian Formation, Mackenzie Mountains, Yukon and Northwest Territories: Current Research, Part B: Geological Survey of Canada Paper 82–1B, p. 83–92.

Gabrielse, H., 1972, Younger Precambrian of the Canadian Cordillera: American Journal of Science, v. 272, p. 521–536, doi:10.2475/ajs.272.6.521.

Gehling, J.G., 1999, Microbial mats in terminal Proterozoic siliciclastics: Ediacaran death masks: Palaios, v. 14, p. 40–57, doi:10.2307/3515360.

Gill, B.C., Lyons, T.W., Young, S.A., Kump, L.R., Knoll, A.H., and Saltzman, M.R., 2011, Geochemical evidence for widespread euxinia in the later Cambrian ocean: Nature, v. 469, p. 80–83, doi:10.1038/nature09700.

Gomes, M.L., and Hurtgen, M.T., 2015, Sulfur isotope fractionation in modern euxinic systems: Implications for paleoenvironmental reconstructions of paired sulfate-sulfide isotope records: Geochimica et Cosmochimica Acta, v. 157, p. 39–55, doi:10.1016/j.gca.2015.02.031.

Gordey, S.P., and Anderson, R.G., 1993, Evolution of the Northern Cordilleran Miogeocline, Nahanni Map Area (105I), Yukon and Northwest Territories: Geological Survey of Canada Memoir 428, 214 p.

Gordey, S.P., Roots, C.F., Martel, E., MacDonald, J., Fallas, K.M., and MacNaughton, R.B., 2011, Bedrock Geology, Mount Eduni (106A), Northwest Territories: Geological Survey of Canada Open-File 6594, scale 1:250,000.

Gorjan, P., Veevers, J.J., and Walter, M.R., 2000, Neoproterozoic sulfur-isotope variation in Australia and global implications: Precambrian Research, v. 100, p. 151–179, doi:10.1016/S0301-9268(99)00073-X.

Grazhdankin, D., 2014, Patterns of evolution of the Ediacaran soft-bodied biota: Journal of Paleontology, v. 88, p. 269–283, doi:10.1666/13-072.

Grieshaber, M.K., and Völkel, S., 1998, Animal adaptations for tolerance and exploitation of poisonous sulfide: Annual Review of Physiology, v. 60, p. 33–53, doi:10.1146/annurev.physiol.60.1.33.

Grieshaber, M.K., Hardewig, I., Kreutzer, U., and Pörtner, H.-O., 1994, Physiological and metabolic responses to hypoxia in invertebrates: Reviews of Physiology, Biochemistry and Pharmacology, v. 125, p. 43–147, doi:10.1007/BFb0030909.

Grotzinger, J.P., Bowring, S.A., Saylor, B.Z., and Kaufman, A.J., 1995, Biostratigraphic and geochronologic constraints on early animal evolution: Science, v. 270, p. 598–604, doi:10.1126/science.270.5236.598.

Halverson, G.P., Wade, B.P., Hurtgen, M.T., and Barovich, K.M., 2010, Neoproterozoic chemostratigraphy: Precambrian Research, v. 182, p. 337–350, doi:10.1016/j.precamres.2010.04.007.

Hayes, J.M., Lambert, I.B., and Strauss, H., 1992, The sulfur-isotopic record *in* Schopf, J.W., and Klein, C., eds., The Proterozoic Biosphere, A Multidisciplinary Study: Cambridge, UK, Cambridge University Press, p. 129–132.

Helz, G.R., Miller, C.V., Charnock, J.M., Mosselmans, J.F.W., Pattrick, R.A.D., Garner, C.D., and Vaughan, D.J., 1996, Mechanism of molybdenum removal from the sea and its concentration in black shales: EXAFS evidence: Geochimica et Cosmochimica Acta, v. 60, p. 3631–3642, doi:10.1016/0016-7037(96)00195-0.

Hickson, C.J., and Juras, S.J., 1986, Sample contamination by grinding: Canadian Mineralogist, v. 24, p. 585–589.

Hoffman, P.F., and Halverson, G.P., 2011, Neoproterozoic glacial record in the Mackenzie Mountains, northern Canadian Cordillera, *in* Arnaud, E., Halverson, G.P., and Shields-Zhou, G., eds., The Geological Record of Neoproterozoic Glaciations: Geological Society of London Memoir 36, p. 397–412.

Hofmann, H.J., 1981, First record of a late Proterozoic faunal assemblage in the North American Cordillera: Lethaia, v. 14, p. 303–310, doi:10.1111/j.1502-3931.1981.tb01103.x.

Hofmann, H.J., Narbonne, G.M., and Aitken, J.D., 1990, Ediacaran remains from intertillite beds in northwestern Canada: Geology, v. 18, p. 1199–1202, doi:10.1130/0091-7613(1990)018<1199:ERFIBI>2.3.CO;2.

Holland, H.D., 2006, The oxygenation of the atmosphere and oceans: Philosophical Transactions of the Royal Society of London, ser. B, Biological Sciences, v. 361, p. 903–915, doi:10.1098/rstb.2006.1838.

Ivantsov, A.Y., Gritsenko, V.P., Konstantinenko, L.I., and Zakrevskaya, M.A., 2014, Revision of the problematic Vendian macrofossil *Beltanelliformis* (= *Beltanelloides, Nemiana*): Paleontological Journal, v. 48, p. 1415–1440, doi:10.1134/S0031030114130036.

James, N.P., Narbonne, G.M., and Kyser, T.K., 2001, Late Neoproterozoic cap carbonates: Mackenzie Mountains, northwestern Canada: Precipitation and global glacial meltdown: Canadian Journal of Earth Sciences, v. 38, p. 1229–1262, doi:10.1139/e01-046.

Jefferson, C.W., and Parish, R.R., 1989, Late Proterozoic stratigraphy, U-Pb zircon ages, and rift tectonics, Mackenzie Mountains, northwestern Canada: Canadian Journal of Earth Sciences, v. 26, p. 1784–1801, doi:10.1139/e89-151.

Jefferson, C.W., and Ruelle, J.C.L., 1986, The late Proterozoic Redstone Copper Belt, Mackenzie Mountains, Northwest Territories *in* Morin, J.A., ed., Mineral Deposits of Northern Cordillera: Canadian Institute of Mining and Metallurgy Special Volume 37, p. 154–168.

Jimenez Berrocoso, A., MacLeod, K.G., Calvert, S.E., and Elorza, J., 2008, Bottom water anoxia, inoceramid colonization, and benthopelagic coupling during black shale deposition on Demerara Rise (Late Cretaceous western tropical North Atlantic): Paleoceanography, v. 23, p. PA3212, doi:10.1029/2007PA001545.

Johnston, D.T., Poulton, S.W., Goldberg, T., Sergeev, V.N., Podkovyrov, B., Vorob'eva, N.G., Bekker, A., and Knoll, A.H., 2012, Late Ediacaran redox stability and metazoan evolution: Earth and Planetary Science Letters, v. 335–336, p. 25–35, doi:10.1016/j.epsl.2012.05.010.

Johnston, D.T., Poulton, S.W., Tosca, N.J., O'Brien, T., Halverson, G.P., Schrag, D.P., and Macdonald, F.A., 2013, Searching for an oxygenation event in the fossiliferous Ediacaran of northwestern Canada: Chemical Geology, v. 362, p. 273–286, doi:10.1016/j.chemgeo.2013.08.046.

Kah, L.C., and Bartley, J.K., 2011, Protracted oxygenation of the Proterozoic biosphere: International Geology Review, v. 53, p. 1424–1442, doi:10.1080/00206814.2010.527651.

Kenig, F., Hudson, J.D., Damste, J.S.S., and Popp, B.N., 2004, Intermittent euxinia: Reconciliation of a Jurassic black shale with its biofacies: Geology, v. 32, p. 421–424, doi:10.1130/G20356.1.

Knoll, A.H., 2014, Paleobiological perspectives on early eukaryotic evolution: Cold Spring Harbor Perspectives in Biology, v. 6, p. 1–13, doi:10.1101/cshperspect.a016121.

Leavitt, W.D., Halevy, I., Bradley, A.S., and Johnston, D.T., 2013, Influence of sulfate reduction rates on the Phanerozoic sulfur isotope record: Proceedings of the National Academy of Sciences of the United States of America, v. 110, p. 11,244–11,249, doi:10.1073/pnas.1218874110.

Levin, L., Ekau, W., Gooday, A., Jorissen, F., Middelburg, J., Naqvi, W., Neira, C., Rabalais, N., and Zhang, J., 2009a, Effects of natural and human-induced hypoxia on coastal benthos: Biogeosciences Discussions, v. 6, p. 3563–3654, doi:10.5194/bgd-6-3563-2009.

Levin, L.A., Whitcraft, C.R., Mendoza, G.F., Gonzalez, J.P., and Cowie, G., 2009b, Oxygen and organic matter thresholds for benthic faunal activity on the Pakistan margin oxygen minimum zone (700–1100 m): Deep-Sea Research, Part II, Topical Studies in Oceanography, v. 56, p. 449–471, doi:10.1016/j.dsr2.2008.05.032.

Li, C., Love, G.D., Lyons, T.W., Fike, D.A., Sessions, A.L., and Chu, X., 2010, A stratified redox model for the Ediacaran ocean: Science, v. 328, p. 80–83, doi:10.1126/science.1182369.

Li, C., Love, G.D., Lyons, T.W., Scott, C.T., Feng, L., Huang, J., Chang, H., Zhang, Q., and Chu, X., 2012, Evidence for a redox stratified Cryogenian marine basin, Datangpo Formation, South China: Earth and Planetary Science Letters, v. 331, p. 246–256, doi:10.1016/j.epsl.2012.03.018.

Lickorish, W.H., and Simony, P.S., 1995, Evidence for late rifting of the Cordilleran margin outlined by stratigraphic division of the Lower Cambrian Gog Group, Rocky Mountain Main Ranges, British Columbia and Alberta: Canadian Journal of Earth Sciences, v. 32, p. 860–874, doi:10.1139/e95-072.

Link, P.K., Christie-Blick, N., Devlin, W.J., Elston, D.P., Horodyski, R.J., Levy, M., Miller, J.M.G., Pearson, R.C., Prave, A.R., Stewart, J.H., Winston, D., Wright, L.A., and Wrucke, C.T., 1993, Middle and late Proterozoic stratified rocks of the western U.S. Cordillera, Colorado Plateau, and Basin and Range Province, *in* Reed, J.C., Bickford, M.E., Houston, R. S., Link, P.K., Rankin, D.W., Sims, P.K., and Schmus, V., eds., Precambrian: Conterminous U.S.: Boulder, Colorado, Geological Society of America, The Geology of North America, v. C-2, p. 463–595.

Liu, A.G., McIlroy, D., and Brasier, M.D., 2010, First evidence for locomotion in the Ediacara biota from the 565 Ma Mistaken Point Formation, Newfoundland: Geology, v. 38, p. 123–126.

Liu, A.G., Kenchington, C.G., and Mitchell, E.G., 2015, Remarkable insights into the paleoecology of the Avalonian Ediacaran macrobiota: Gondwana Research, v. 27, p. 1355–1380, doi:10.1016/j.gr.2014.11.002.

Lyons, T.W., and Severmann, S., 2006, A critical look at iron paleoredox proxies: New insights from modern euxinic marine basins: Geochimica et Cosmochimica Acta, v. 70, p. 5698–5722, doi:10.1016/j.gca.2006.08.021.

Macdonald, F.A., Schmitz, M.D., Crowley, J.L., Roots, C.F., Jones, D.S., Maloof, A.C., Strauss, J.V., Cohen, P.A., Johnston, D.T., and Schrag, D.P., 2010, Calibrating the Cryogenian: Science, v. 327, p. 1241–1243, doi:10.1126/science.1183325.

Macdonald, F.A., Strauss, J.V., Sperling, E.A., Halverson, G.P., Narbonne, G.M., Johnston, D.T., Kunzmann, M., Schrag, D.P., and Higgins, J.A., 2013, The stratigraphic relationship between the Shuram carbon isotope excursion, the oxygenation of Neoproterozoic oceans, and the first appearance of the Ediacara biota and bilaterian trace fossils in northwestern Canada: Chemical Geology, v. 362, p. 250–272, doi:10.1016/j.chemgeo.2013.05.032.

Macdonald, F.A., Pruss, S.B., and Strauss, S.V., 2014, Trace fossils with spreiten from the late Ediacaran Nama Group, Namibia: Complex feeding patterns five million years before the Precambrian-Cambrian boundary: Journal of Paleontology, v. 88, p. 299–308, doi:10.1666/13-042.

MacNaughton, R.B., and Narbonne, G.M., 1999, Evolution and ecology of Neoproterozoic–Lower Cambrian trace fossils, NW Canada: Palaios, v. 14, p. 97–115, doi:10.2307/3515367.

MacNaughton, R.B., Narbonne, G.M., and Dalrymple, R.W., 2000, Neoproterozoic slope deposits, Mackenzie Mountains, northwestern Canada: Implications for passive-margin development and Ediacaran faunal ecology: Canadian Journal of Earth Sciences, v. 37, p. 997–1020, doi:10.1139/e00-012.

MacNaughton, R., Roots, C.F., and Martel, E., 2008, Neoproterozoic–(?)Cambrian lithostratigraphy, northeast Sekwi Mountain map area, Mackenzie Mountains, Northwest Territories: New data from measured sections: Geological Survey of Canada Current Research 2008–16, p. 1–17.

Maloof, A.C., Porter, S.M., Moore, J.L., Dudas, F.O., Bowring, S.A., Higgins, J.A., Fike, D.A., and Eddy, M.P., 2010, The earliest Cambrian record of animals and ocean geochemical change: Geological Society of America Bulletin, v. 122, p. 1731–1774.

Martel, E., Turner, E.C., and Fischer, B.J., 2011, Geology of the Central Mackenzie Mountains of the Northern Canadian Cordillera: Sekwi Mountain (105P), Mount Eduni (106A), and Northwestern Wrigley Lake (95M) Map Areas, Northwest Territories: Northwest Territories (NWT) Geoscience Office, NWT Special Volume 1, 423 p.

Matabos, M., Tunnicliffe, V., Juniper, S.K., and Dean, C., 2012, A year in hypoxia: Epibenthic community responses to severe oxygen deficit at a subsea observatory in a coastal inlet: PLoS ONE, v. 7, no. 9, p. e45626, doi:10.1371/journal.pone.0045626.

McLennan, S.M., 2001, Relationships between the trace element composition of sedimentary rocks and upper continental crust: Geochemistry Geophysics Geosystems, v. 2, p. 1021, doi:10.1029/2000GC000109.

Narbonne, G.M., 1994, New Ediacaran fossils from the Mackenzie Mountains, northwestern Canada: Journal of Paleontology, v. 68, p. 411–416.

Narbonne, G.M., and Aitken, J.D., 1990, Ediacaran fossils from the Sekwi Brook area, Mackenzie Mountains, northwestern Canada: Palaeontology, v. 33, p. 945–980.

Narbonne, G.M., and Aitken, J.D., 1995, Neoproterozoic of the Mackenzie Mountains, northwestern Canada: Precambrian Research, v. 73, p. 101–121, doi:10.1016/0301-9268(94)00073-Z.

Narbonne, G.M., and Gehling, J.G., 2003, Life after Snowball: The oldest complex Ediacaran fossils: Geology, v. 31, p. 27–30, doi:10.1130/0091-7613(2003)031<0027:LASTOC>2.0.CO;2.

Narbonne, G.M., Xiao, S., and Shields, G., 2012, The Ediacaran Period, *in* Gradstein, F., Ogg, J., Schmitz, M.D., and Ogg, G., eds., Geologic Timescale 2012: Amsterdam, Elsevier, p. 427–449.

Narbonne, G.M., Laflamme, M., Trusler, P.W., Dalrymple, R.W., and Greentree, C., 2014, Deep-water Ediacaran fossils from northwestern Canada: Taphonomy, ecology, and evolution: Journal of Paleontology, v. 88, p. 207–223, doi:10.1666/13-053.

Och, L.M., and Shields-Zhou, G.A., 2012, The Neoproterozoic oxygenation event: Environmental perturbations and biogeochemical cycling: Earth-Science Reviews, v. 110, p. 26–57, doi:10.1016/j.earscirev.2011.09.004.

Partin, C., Bekker, A., Planavsky, N., Scott, C., Gill, B., Li, C., Podkovyrov, V., Maslov, A., Konhauser, K., and Lalonde, S., 2013, Large-scale fluctuations in Precambrian atmospheric and oceanic oxygen levels from the record of U in shales: Earth and Planetary Science Letters, v. 369–370, p. 284–293, doi:10.1016/j.epsl.2013.03.031.

Patzkowsky, M.E., and Holland, S.M., 2012. Stratigraphic Paleobiology: Chicago, Illinois, The University of Chicago Press, 256 p.

Planavsky, N.J., McGoldrick, P., Scott, C.T., Li, C., Reinhard, C.T., Kelly, A.E., Chu, X., Bekker, A., Love, G.D., and Lyons, T.W., 2011, Widespread iron-rich conditions in the mid-Proterozoic ocean: Nature, v. 477, p. 448–451, doi:10.1038/nature10327.

Poulton, S.W., and Canfield, D.E., 2005, Development of a sequential extraction procedure for iron: Implications for iron partitioning in continentally derived particulates: Chemical Geology, v. 214, p. 209–221, doi:10.1016/j.chemgeo.2004.09.003.

Poulton, S.W., and Canfield, D.E., 2011, Ferruginous conditions: A dominant feature of the ocean through Earth's history: Elements, v. 7, p. 107–112, doi:10.2113/gselements.7.2.107.

Poulton, S.W., and Raiswell, R., 2002, The low-temperature geochemical cycle of iron: From continental fluxes to marine sediment deposition: American Journal of Science, v. 302, p. 774–805, doi:10.2475/ajs.302.9.774.

Raiswell, R., and Canfield, D.E., 1998, Sources of iron for pyrite formation in marine sediments: American Journal of Science, v. 298, p. 219–245, doi:10.2475/ajs.298.3.219.

Raiswell, R., Newton, R., and Wignall, P.B., 2001, An indicator of water-column anoxia: Resolution of biofacies variations in the Kimmeridge Clay (Upper Jurassic, U.K.): Journal of Sedimentary Research, v. 71, p. 286–294, doi:10.1306/070300710286.

Raiswell, R., Newton, R., Bottrell, S.H., Coburn, P.M., Briggs, D.E.G., Bond, D.P.G., and Poulton, S.W., 2008, Turbidite depositional influences on the diagenesis of Beecher's Trilobite Bed and the Hunsruck Slate; sites of soft tissue pyritization: American Journal of Science, v. 308, p. 105–129, doi:10.2475/02.2008.01.

Reinhard, C.T., Planavsky, N.J., Robbins, L.J., Partin, C.A., Gill, B.C., Lalonde, S.V., Bekker, A., Konhauser, K.O., and Lyons, T.W., 2013, Proterozoic ocean redox and biogeochemical stasis: Proceedings of the National Academy of Sciences of the United States of America, v. 110, p. 5357–5362, doi:10.1073/pnas.1208622110.

Rice, A., Tait, J., and Anderson, M., 2009, Use of tungsten carbide disc-mill in geochemistry: No evidence of contamination, *in* Geophysical Research Abstracts, v. 11, p. 9350.

Rooney, A.D., Macdonald, F.A., Strauss, J.V., Dudas, F.O., Hallmann, C., and Selby, D., 2014, Re-Os geochronology and coupled Os-Sr isotope constraints on the Sturtian snowball Earth: Proceedings of the National Academy of Sciences of the United States of America, v. 111, p. 51–56, doi:10.1073/pnas.1317266110.

Rooney, A.D., Strauss, J.V., Brandon, A.D., and Macdonald, F.A., 2015, A Cryogenian chronology: Two long-lasting, synchronous glaciations: Geology, v. 43, p. 459–462, doi:10.1130/G36511.1.

Ross, G.M., 1991, Tectonic setting of the Windermere Supergroup revisited: Geology, v. 19, p. 1125–1128, doi:10.1130/0091-7613(1991)019<1125:TSOTWS>2.3.CO;2.

Ross, G.M., McMechan, M.E., and Hein, F.J., 1989, Proterozoic history: Birth of the miogeocline, *in* Ricketts, B.D., ed., Western Canada Sedimentary Basin—A Case History: Calgary, Canadian Society of Petroleum Geologists, p. 79–104.

Ross, G.M., Bloch, J.D., and Krouse, H.R., 1995, Neoproterozoic strata of the southern Canadian Cordillera and the isotopic evolution of seawater sulfate: Precambrian Research, v. 73, p. 71–99, doi:10.1016/0301-9268(94)00072-Y.

Santos, S.L., and Simon, J.L., 1980, Response of soft-bottom benthos to annual catastrophic disturbance in a south Florida estuary: Marine Ecology Progress Series, v. 3, p. 347–355, doi:10.3354/meps003347.

Savrda, C.E., Bottjer, D.J., and Gorsline, D.S., 1984, Development of a comprehensive oxygen-deficient marine biofacies model: Evidence from Santa Monica, San Pedro, and Santa Barbara Basins, California Continental Borderland: American Association of Petroleum Geologists Bulletin, v. 68, p. 1179–1192.

Schieber, J., 2003, Simple gifts and buried treasures—Implications of finding bioturbation and erosion surfaces in black shales: The Sedimentary Record, v. 1, p. 4–8.

Schmitz, M.D., 2012, Radiometric ages used in GTS2012, Appendix 2, *in* Gradstein, F., Ogg, J., Schmitz, M.D., and Ogg, G., eds., Geologic Timescale 2012: Amsterdam, Elsevier, p. 1045–1082.

Scott, C., and Lyons, T.W., 2012, Contrasting molybdenum cycling and isotopic properties in euxinic versus non-euxinic sediments and sedimentary rocks: Refining the paleoproxies: Chemical Geology, v. 324, p. 19–27, doi:10.1016/j.chemgeo.2012.05.012.

Shen, Y., Knoll, A.H., and Walter, M.R., 2003, Evidence for low sulphate and anoxia in a mid-Proterozoic marine basin: Nature, v. 423, p. 632–635, doi:10.1038/nature01651.

Shen, Y., Zhang, T., and Hoffman, P.F., 2008, On the coevolution of Ediacaran oceans and animals: Proceedings of the National Academy of Sciences of the United States of America, v. 105, p. 7376–7381, doi:10.1073/pnas.0802168105.

Sim, M.S., Bosak, T., and Ono, S., 2011, Large sulfur isotope fractionation does not require disproportionation: Science, v. 333, p. 74–77, doi:10.1126/science.1205103.

Sperling, E.A., Halverson, G.P., Knoll, A.H., Macdonald, F.A., and Johnston, D.T., 2013, A basin redox transect at the dawn of animal life: Earth and Planetary Science Letters, v. 371, p. 143–155, doi:10.1016/j.epsl.2013.04.003.

Sperling, E.A., Rooney, A.D., Hays, L., Sergeev, V.N., Vorob'eva, N.G., Sergeeva, N.D., Selby, D., Johnston, D.T., and Knoll, A.H., 2014, Redox heterogeneity of subsurface waters in the Mesoproterozoic ocean: Geobiology, v. 12, p. 373–386, doi:10.1111/gbi.12091.

Sperling, E.A., Wolock, C.J., Morgan, A.S., Gill, B.C., Kunzmann, M., Halverson, G.P., Macdonald, F.A., Knoll, A.H., and Johnston, D.T., 2015, Statistical analysis of iron geochemical data suggests limited late Proterozoic oxygenation: Nature, v. 523, p. 451–454, doi:10.1038/nature14589.

Thomson, D., Rainbird, R.H., Planavsky, N., Lyons, T.W., and Bekker, A., 2015, Chemostratigraphy of the Shaler Supergroup, Victoria Island, NW Canada: A record of ocean composition prior to the Cryogenian glaciations: Precambrian Research, v. 263, p. 232–245, doi:10.1016/j.precamres.2015.02.007.

Thorkelson, D.J., 2000, Geology and Mineral Occurrences of the Slats Creek, Fairchild Lake, and "Dolores Creek" Areas, Wernecke Mountains, Yukon Territory (106D/16, 106C/13, 106C/14): Exploration and Geological Services Division, Yukon Region, Indian and Northern Affairs Canada, Bulletin 10, 80 p.

Tribovillard, N., Algeo, T.J., Lyons, T., and Riboulleau, A., 2006, Trace metals as paleoredox and paleoproductivity proxies: An update: Chemical Geology, v. 232, p. 12–32, doi:10.1016/j.chemgeo.2006.02.012.

Turekian, K.K., and Wedepohl, K.H., 1961, Distribution of the elements in some major units of Earth's crust: Geological Society of America Bulletin, v. 72, p. 175–192, doi:10.1130/0016-7606(1961)72[175:DOTEIS]2.0.CO;2.

Turner, E.C., Roots, C.F., MacNaughton, R.B., Long, D.G.F., Fischer, B.J., Gordey, S.P., Martel, E., and Pope, M.C., 2011, Chapter 3. Stratigraphy, *in* Martel, E., Turner, E.C., and Fischer, B.J., eds., Geology of the Central Mackenzie Mountains of the Northern Canadian Cordillera, Sekwi Mountain (105P), Mount Eduni (106A), and Northwestern Wrigley Lake (95M) Map-Areas, Northwest Territories: Yellowknife, Northwest Territories Geoscience Office, p. 31–192.

Wood, R.A., Poulton, S.W., Prave, A.R., Hoffmann, K.H., Clarkson, M.O., Guilbaud, R., Lyne, J.W., Tostevin, R., Bowyer, F., and Penny, A.M., 2015, Dynamic redox conditions control late Ediacaran metazoan ecosystems in the Nama Group, Namibia: Precambrian Research, v. 261, p. 252–271, doi:10.1016/j.precamres.2015.02.004.

Xiao, S., and Laflamme, M., 2009, On the eve of animal radiation: Phylogeny, ecology and evolution of the Ediacaran biota: Trends in Ecology & Evolution, v. 24, p. 31–40, doi:10.1016/j.tree.2008.07.015.

Yonkee, W.A., Dehler, C.D., Link, P.K., Balgord, E.A., Keeley, J.A., Hayes, D.S., Wells, M.L., Fanning, C.M., and Johnston, S.M., 2014, Tectono-stratigraphic framework of Neoproterozoic to Cambrian strata, west-central US: Protracted rifting, glaciation, and evolution of the North American Cordilleran margin: Earth-Science Reviews, v. 136, p. 59–95, doi:10.1016/j.earscirev.2014.05.004.

Zhou, C., and Xiao, S., 2007, Ediacaran $\delta^{13}C$ chemostratigraphy of South China: Chemical Geology, v. 237, p. 89–108, doi:10.1016/j.chemgeo.2006.06.021.

Science Editor: Christian Koeberl
Associate Editor: Brian R. Pratt

Manuscript Received 1 April 2015
Revised Manuscript Received 11 July 2015
Manuscript Accepted 15 September 2015

Printed in the USA